

NPS ARCHIVE
1969
FLETCHER, M.

SURFACE WAKE OF A CIRCULAR CYLINDER IN
DILUTE AQUEOUS SOLUTIONS OF POLY (ETHYLENE
OXIDE)

by

Michael Henry Fletcher

United States Naval Postgraduate School



THESIS

SURFACE WAKE OF A CIRCULAR CYLINDER IN DILUTE
AQUEOUS SOLUTIONS OF POLY (ETHYLENE OXIDE)

by

Michael Henry Fletcher

T132822

June 1969

*This document has been approved for public re-
lease and sale; its distribution is unlimited.*

al Postgraduate School
er, California 93940

Surface Wake of a Circular Cylinder in Dilute
Aqueous Solutions of Poly(ethylene oxide)

by

Michael Henry Fletcher
Lieutenant (junior grade), United States Navy
B.S., United States Naval Academy, 1968

Submitted in partial fulfillment of the
requirements for the degree of

MASTER OF SCIENCE IN PHYSICS

from the

NAVAL POSTGRADUATE SCHOOL
June 1969

ABSTRACT

The wake formed by surface-piercing circular cylinders towed through 0, 100, and 200 parts per million (by weight) aqueous solutions of Poly(ethylene oxide), Polyox WSR-301, was examined photographically. Cylinder diameters ranged from 1/4 in. to 2 in.; Froude numbers from 0.6 to 10. Measurements of spray height and ventilation pocket depth were made. No significant alteration of pocket depth with polymer concentration was observed; however, the spray height was reduced by increasing the Polyox concentration. Qualitative differences between the wakes of cylinders in Polyox solutions and those in water were (1) a serrated separation line characterized the ventilation pocket of the polymer solutions as opposed to the straight separation line of water, (2) the striated appearance of the pocket walls in Polyox instead of the clear, smooth walls in water, (3) the coherence displayed by the spray in Polyox instead of the random character of the spray in water, and (4) the larger and more irregularly shaped bubbles in Polyox as opposed to those in water.

TABLE OF CONTENTS

I. INTRODUCTION -----	7 /
II. APPARATUS AND EXPERIMENTAL PROCEDURE -----	11 /
A. APPARATUS -----	11
B. PROCEDURE -----	13 /
C. MIXING THE POLYMER SOLUTION -----	14
D. DEVELOPMENT OF PARAMETERS -----	15 /
III. RESULTS -----	17
A. SPRAY HEIGHT -----	17 /
B. VENTILATION POCKET DEPTH -----	18
C. QUALITATIVE EFFECTS -----	19
IV. CONCLUSIONS -----	21
APPENDIX A GRAPHS -----	23
APPENDIX B FIGURES -----	37
BIBLIOGRAPHY -----	55
INITIAL DISTRIBUTION LIST -----	58
DD FORM 1473 -----	59

LIST OF SYMBOLS

- d = Diameter of cylinder
- F_d = Froude number based on diameter
- F_h = Froude number based on ventilation pocket depth
- g = Acceleration due to gravity
- h_{po} = Depth of ventilation pocket measured from undisturbed level
- h_u = Height of spray
- ρ = Mass density of fluid
- V = Speed of the moving cylinder

ACKNOWLEDGEMENTS

The author wishes to thank Milt Andrews, Bill Smith, Bob Moeller, and Barney Taylor for their technical assistance in this research.

I. INTRODUCTION

The drag and noise reducing effect of dilute solutions of long chain molecules (polymers) has been vigorously investigated in recent years. Early studies consisted of examining the flow rate of these solutions through cylindrical pipes [1-16]. From these experiments, it was concluded that for pipe flow:

- 1) No drag reduction occurs until the flow characteristics change from laminar to turbulent [16].
- 2) The amount of drag reduction increases with the Reynolds number of the flow and with the molecular weight of the polymer additive [5,10].
- 3) The thickness of the viscous sublayer increases with the concentration of the polymer [3,12,15].

The results of experimental work with rotary disks immersed in dilute polymer solutions confirmed the results of pipe flow with respect to molecular weight; and, in addition, demonstrated that maximum drag reduction occurred with linear polymers. The longer the molecule; the greater the corresponding drag reduction [17].

Early attempts to explain the friction and turbulence reducing mechanism of dilute polymer solutions included the proposals of slip at the wall [1,12], delayed transition to a turbulent boundary layer [6,12], and anisotropic viscosity [30]. Another, and currently most popular, theory attributes the drag reduction to the viscoelastic properties of the solution. The polymer, according to this theory,

affects the viscous sublayer [4,6,8], the flow relaxation time [4,6,7,8], the turbulent energy spectra [6,8,14,18], and the production and dissipation of turbulent energy [6,8,14].

Streamlined bodies in turbulent flow of polymer solutions were examined and similar drag reduction was noted [18]. However, it was found that after a critical concentration the drag on a streamlined body increased over that experienced in water [19,20]. This increased drag was attributed to earlier separation of the boundary layer caused by the complete laminarization of the boundary layer by the high concentration of polymer. The earlier separation causes a larger wake than that in water alone thus augmenting the drag.

The motion of blunt bodies through polymer solutions has also been investigated. Experiments with spheres [22,23,24], and also with cones, cylinders, and disks [24] freely falling through polymer solutions were conducted. The results show that drag reduction takes place for those bodies with a moveable separation point, but no reduction was observed on those with fixed separation points. A rearward displacement of the separation point on those bodies with moveable points was noted in polymer solutions [24].

At the Naval Postgraduate School, experiments with various size spheres, polymer types, and concentrations have been conducted with freely falling spheres [25,26,27]. The conclusions reached for the polymer Poly(ethylene oxide) (Polyox WSR-301), which was the most effective drag reducer, were that for spheres:

- 1) No drag reduction was detected for any concentration of polymer for Reynolds numbers (based on the viscosity of water) below 10^4 . Indeed, in this region, an increase of drag with polymer concentration was observed [25].

2) For water Reynolds numbers above 10^4 , at a given concentration, drag reduction increased with Reynolds number (as in pipe flow).

3) For water Reynolds numbers less than 10^5 , maximum drag reduction occurred in a solution of 100 parts per million by weight (wppm) [26].

4) For Reynolds numbers above 10^5 , a 200 wppm solution exhibited better drag reduction than the 100 wppm solution [27].

A proposed explanation for the reduced drag of spheres states that, for wake dominated flow, the polymer solution displaces the point of separation rearward thus reducing wake size and drag [25].

Experiments on towed cylinders have shown that cylinders exhibit behavior similar to freely falling spheres [28,29]:

1) Drag augmentation occurred, drag increasing with increasing polymer concentration, for flows with water Reynolds numbers less than 10^4 .

2) Above a Reynolds number of 10^4 , drag reduction occurs; and, at constant concentration, this reduction increases with increasing Reynolds number.

3) Maximum drag reduction was obtained in a 100 wppm Polyox solution.

Experimental work has been done to find the effects of dilute polymer solutions on cavitation inception with the conclusion that a definite hindering of inception was observed. This effect was greatest for solutions of 50 wppm Polyox WSR-301 [32].

Some effects of the polymer solutions on the spray and surface wake caused by a towed surface-piercing strut have been reported [29].

A reduction in the size of the surface wake and a tendency for the spray to form sheets instead of droplets were qualitatively noted.

Extensive work on the spray and ventilation (the formation of an air-filled pocket behind a surface piercing object) of towed bodies in water has shown that three characteristic flow patterns exist depending on the Froude number [33]. These are:

- 1) At Froude numbers approaching zero, the deformation of the surface is negligibly small.
- 2) For flow characterized by Froude numbers between zero and one, the typical wave pattern is formed with transverse and lateral waves originating at the leading and trailing edges of the body.
- 3) Spray and possibly ventilation dominate the flow for Froude numbers greater than one. (See Fig. 1.)

The effect of a polymer additive on the flow around surface-piercing bodies would be of interest in the areas of hydrofoil development and periscope detection or in many areas where a surface-piercing body is utilized.

II. APPARATUS AND EXPERIMENTAL PROCEDURE

A. APPARATUS

The experiment reported herein was performed in the circular towing tank at the Naval Postgraduate School. This tank has a seven-foot outer diameter, four-foot inner diameter, and a wall height of eighteen inches. (See Fig. 2.) A window, through which pictures could be taken, was installed in the outer wall of the tank. The window (26" x 18" x 1" plexiglass) was mounted in an aluminum frame bolted to the tank. A one-inch thickness was chosen to prevent warping of the window by water pressure thereby aiding the optical fidelity of the photographs. (See Fig. 3.) A Craftsman 1 1/2 horsepower electric motor supplied motive power, through a pulley and belt combination and an Alliance Masterreducer reduction gear, to an aluminum T-beam towing arm. Pulley ratios possible were 1/3.7, 1/1.5, 1.5/1, 3.7/1. The cylinders were mounted on this arm equidistant from the sidewalls of the tank so that they traced out a circle 16.74 feet in length. The speed of rotation of the arm could be varied by a potentiometer motor control and by changing pulley ratios.

The ranges of parameters covered in this experiment were: speeds from 80 to 200 cm/sec; Froude numbers from 0.6 to 10; Reynolds numbers from 6.3×10^3 to 7.1×10^4 . Cylinders used were of 1/4", 1/2", 1", and 2" diameter.

The cylinders were made of aluminum in either solid bar or pipe form. These were polished to present a smooth surface to the fluid flow and mounted in a clamp which was bolted to the towing arm. A

cylinder was mounted so that the axis of the cylinder was normal to the water surface. For all cylinders but the two-inch diameter one, eight inches of the cylinder were immersed leaving five inches between the bottom of the cylinder and the floor of the tank. At this depth there appeared to be little influence of the floor on the spray and ventilation pocket of the cylinders for the speeds used in this experiment. The maximum speed attainable was limited by the necessity of keeping the ventilation pocket out of the influence of the cylinder bottom. This influence is indicated by the obscuring of the bottom of the pocket in a flurry of cavitation bubbles. (See Figs. 6 and 7.) The two-inch cylinder was mounted so as to be only 3 1/2 inches from the floor of the tank. This was probably too close, but since this cylinder was most likely too large for the channel of the tank anyway, no effort was made to alter this situation.

The speed of the cylinders in passing the window was determined by means of a cam and microswitch assembly. (Fig. 4.) The cam, fixed to the towing arm, momentarily depressed a microswitch as the cylinder approached the window. The 1.5 volt pulse from this switch started a Hewlett-Packard model 5233L electronic counter. As the cylinder came to the other side of the window, a second microswitch was tripped; and another 1.5 volt pulse stopped the counter. The time to traverse the window was then read directly from the counter. By direct measurement, the distance traveled by the cylinder between microswitch contacts was found to be 51.6 cm and the average velocity obtained by dividing this distance by the time. Since terminal velocity appeared to be achieved at the start of a run within about 3 feet, and since the cylinders traveled approximately two thirds of the way around

the tank (about eleven feet) before reaching the window, the assumption that the velocity was constant during passage across the window is a reasonable one.

The cam arrangement was also used to trip a third microswitch which was located between the timing switches. This third switch closed the contact which triggered a Strobex model 121 strobe light. This light provided illumination for the photographs. The best results were obtained by attaching a white paper reflector to the strobe light and using the indirect reflected light to illuminate cylinder and wake. (See Fig. 5.)

A Graflex camera with Polaroid attachment was used for the photography. It was mounted on a laboratory jack which was attached to a slotted aluminum beam. The beam was fitted to the tank by means of a hinge. With this set-up, the camera could be moved vertically by the jack or slid along the beam for either close or distant pictures. The hinge permitted the beam to swing upward so that photos could be taken from above. The film used was Polaroid, type 47, 3000 speed, black and white. With the indirect lighting, best results were obtained with an f-stop of 4.5. The camera was used in the open-shuttered mode with the strobe light providing the exposure time.

B. PROCEDURE

A routine was developed for taking data as rapidly as possible.

- 1) The tank was filled with water or Polyox solution.
- 2) The camera was mounted on its moveable beam and set for time exposure. Focusing was accomplished by placing a focusing back on the open-shuttered Graflex and focusing directly on the cylinder in the tank.

3) The counter and strobe light were turned on, and the strobe light with reflector was placed directly above the window as shown in Fig. 5.

4) The cylinder was then adjusted for the desired speed by running the cylinder continuously and setting the motor speed control for a speed slightly higher than the desired speed. This was necessary since the adjustment was made in a moving fluid. The larger drag experienced in quiescent fluid during the data run would slow the cylinder to the proper speed. After practice in the different solutions, a feel for the required speed control setting was developed.

5) The cylinder was set in a position approximately one quarter to one third of the way around the tank beyond the window.

6) All lights were turned off, and the camera shutter was opened.

7) The motor was started. After the cylinder passed the window, the motor was stopped and the shutter closed. The lights were then turned on and a wire screen placed in the tank to aid in damping the fluid motion. The exposed picture was then developed, taken out of the camera, and numbered. The time interval from the counter and photo number were then recorded in the data book. By that time, the tank was ready for another run.

C. MIXING THE POLYMER SOLUTION

Poly(ethylene oxide), Polyox WSR-301, manufactured by Union Carbide, was used in this research because of its well demonstrated drag reducing properties. Mixing the polymer in water was accomplished by first suspending either 80 or 160 grams of Polyox, depending on whether a 100 wppm or 200 wppm solution was wanted, in approximately 600 ml. of Polyglycol (P-400, Dow Chemical). The suspension of Polyox in Polyglycol

before mixing with water is necessary; for, if Polyox were added directly to water, it would form globules which dissolve very slowly. The suspension was then added slowly to the stream of water from the hose used to fill the tank. The best mixes resulted when the suspension was dripped into the tank next to the submerged end of the hose. With the end of the hose just submerged, the motion of the entering water could disperse the suspension effectively; and also the amount of air entering the fluid was kept at a minimum. This is desirable since oxygen degrades the effectiveness of the polymer. Once in the tank, the Polyox tends to form globules and precipitate to the bottom. To prevent this, a cylinder was towed through the mix until a uniform solution was attained. All data in this experiment was taken within 12 hours of mixing to reduce any errors introduced by the time degradation of the solution.

D. DEVELOPMENT OF PARAMETERS

The derivation of parameters to describe the spray and ventilation formed by a surface-piercing cylinder follows the development of Hoerner [33]. (See Fig. 1.)

The theoretical height which spray can achieve if scooped up by some ideal, frictionless method can be calculated by setting the potential energy per unit mass of water at maximum height equal to the kinetic energy per unit mass of the free stream:

$$\rho g h_u = \frac{1}{2} \rho V^2.$$

This equation can be solved for h_u to give

$$h_u = \frac{V^2}{2g},$$

where h_u is the spray height, V is the speed, ρ is the mass density of

water, and g is the acceleration due to gravity. The actual height of spray will be less than this because of friction effects in the water itself and between the water and the cylinder wall, and because the shape of the cylinder allows water to flow around it. A plot of $h_u/(V^2/2g)$ versus F_d should, therefore, be meaningful in describing the effectiveness of the cylinder spray phenomenon.

By virtue of its motion, a cylinder moving through water sets up a hydrodynamic pressure field. In the region to the sides of and behind the cylinder the pressure may be negative. If the cylinder pierces the water-air interface, the atmospheric pressure forces the water surface down into any negative pressure regions until a balance is achieved between the sum of the hydrostatic pressure at a given depth (h) plus the hydrodynamic pressure (p) and the atmospheric pressure ($p_{atm.}$). Thus,

$$\rho gh + p = p_{atm.}$$

The maximum depth in the pocket (h_{po}) is reached where the dynamic pressure is a minimum (p_{po}) so that

$$h_{po} = (p_{atm} - p_{po})/\rho g.$$

This depth can be used to define a Froude number,

$$F_h = V/\sqrt{gh_{po}}.$$

Experimental results in water [33] have shown that F_h is a constant depending only on the shape of the body. It is 1.8 for a circular cylinder and 1.4 for a flat plate. If F_h is a constant, then a plot of h_{po} versus V^2 should yield a straight line with slope $F_h^2 g$. This plot can be used to characterize the effect of Polyox on the depth of the ventilation pocket.

III. RESULTS

A. SPRAY HEIGHT

Graph 8 displays the data obtained in water both in this experiment and in work done by Hoerner [33]. Graphs 9 and 10 show the results obtained for solutions of the polymer. Graphs 11 through 14 show these results plotted for each cylinder as a function of concentration of polymer.

Graph 8 shows clearly the scatter of the data observed for the one- and two-inch cylinders in water. In Graphs 9 and 10, it is seen that the additive tended to reduce this scatter for the one-inch cylinder. However, the data for the two-inch cylinder still exhibited scatter in all solutions.

These Graphs also illustrate the tendency of the data for each individual cylinder to lie along its own line, characterized by a downward slope with increasing Froude number. At a given Froude number, the larger the cylinder diameter the closer h_u is to the theoretical height in all solutions. This size effect is apparent in the data of Hoerner only at higher values of F_d .

The most significant effect of the additive is the reduction of spray height as the concentration of the polymer increases. The scatter in the data for the one- and two-inch cylinders for 100 wppm (Graph 9) does not allow any definite statements concerning this reduction for these cylinder sizes at this concentration; however, in 200 wppm, the spray height of all cylinders is noticeably reduced. It can be seen, in Graphs 11 through 14, that the value of $h_u/(V^2/2g)$ in the 100 wppm solution is uniformly (i.e., independent of F_d) lower

than that in water by approximately 10%. In the 200 wppm solution the reduction has increased to approximately 30% of the water value.

Careful study of the data of Graphs 8 through 10 for the two-inch cylinder, the data of Graphs 9 and 10 for the half-inch cylinder, and that of Graph 8 for the one-inch and quarter-inch cylinders will reveal a possible reversal of slope from negative to positive as F_d approaches zero. This reversal may be merely an optical illusion due to the data scatter. If this reversal is real, then the steepness of the slopes in this region could account for the extreme scatter observed. A third alternative is that this reversal is real but is due to interference effects in the tank.

B. VENTILATION POCKET DEPTH

Graph 1 gives the data for ventilation pocket depth recorded in this experiment and, along with Graphs 2 through 7, shows the slopes corresponding to an experimentally determined F_h of 1.8 for circular cylinders and 1.4 for flat plates [33]. Graphs 2 and 3 display those measurements made in the polymer solutions. The data is replotted in Graphs 4 through 7 for each cylinder as a function of polymer concentration.

Graph 1 shows the large amount of scatter in the pocket depth measurements especially for the quarter-inch cylinder. An accurate determination of the depth of the pocket for this cylinder was hindered by the vortex shedding and corresponding lift oscillations that this cylinder exhibited, especially at higher speeds. (See Fig. 29.) These oscillations tended to mask the actual pocket depth.

As shown in Graphs 2 and 3 the polymer slightly reduced the magnitude of the scatter.

The influence of the size of the cylinder on the pocket depth can be seen in Graphs 1 through 3. Here the two-inch cylinder demonstrates a tendency to follow the flat plate slope ($F_h = 1.4$) at lower velocities while the other cylinders tend to follow the slope for an F_h of 1.8. The slope of the data in the Polyox solutions was slightly reduced from that of water although the difference in slope is within the limits of data scatter.

An interesting, though elusive, effect was observed on 30 April 1969, for the one-inch cylinder at speeds near 158 cm/sec. At speeds near this, although the spray was fully developed, no ventilation pocket was formed. (See Figs. 20 & 21). Three pictures were taken of this effect. These pictures and the fact that no bubbles were seen under the water in the cylinder's wake tend to show that this is a steady pattern rather than a momentary collapse of the pocket at the instant the pictures were taken. Even though it was not possible to reproduce this complete disappearance of the pocket in subsequent data runs, a slight dip in pocket depth at velocities near 158 cm/sec can be seen in Graph 3.

C. QUALITATIVE EFFECTS

Attention is called to Figs. 6 through 35 in Appendix B. Both Polyox solutions had dramatic effects on the appearance of the spray and ventilation pockets of all cylinders. (See Figs. 34 & 35.) Whereas the spray in water displayed very little cohesion, especially at higher speeds when droplets would form at the peak of the spray, the polymer solutions caused the spray to form sheets which tended to persist even in the form of large bubbles on the water surface in the cylinder wake. (See Fig. 26.) The bubbles, formed as air was trapped

by falling spray and by the fluctuations of the ventilation pocket especially at the bottom of the pocket, also had a marked difference in appearance in the Polyox solutions. In Polyox, these bubbles were large and irregularly shaped. The water bubbles were, for the most part, much smaller and spherical in shape. (See Figs. 16 & 18.) In the polymer solutions, the ventilation pockets were marked by striations so that the separation line on the cylinder had a serrated appearance; while the water separation line was straight in almost all cases as predicted by theory. (See Figs. 34 & 35.) Similar separation lines and striations were reported by Brennan [34] for fully cavitating flow about completely submerged spheres and other body shapes in polymer solutions. An attempt was made to measure the distance between serrations as a function of cylinder speed and polymer concentration; however, this distance seemed to vary with no definite pattern thus ruling out accurate measurement. The ability to produce a regular serrated separation line with constant serration size appears to be a function of how the polymer solution is mixed and aged [35].

IV. CONCLUSIONS

The technique used in this experiment to measure spray height and ventilation pocket depth by means of photography gave excellent results, but were somewhat tedious. For examining the pocket and spray shapes and for studying the separation line, the technique is particularly well suited.

Qualitatively, the Polyox solutions altered the wake from that of water in various ways. The water forming the spray and ventilation pocket had a tendency to resist deformation so that the flow pattern had a smoother appearance. The spray took on a glassy look, and the ventilation pocket tended to fluctuate less than it did in water; so that a smaller amount of air was admitted into the solution in the form of bubbles. These bubbles were large, irregularly shaped, and glassy in appearance. The Polyox also altered the separation line of the ventilation pocket from a straight line, as in water, to a serrated line. The smooth ventilation pocket of water became marked by horizontal striations in the polymer solutions. These striations emanated from the peaks of the serrations in the separation line.

The depth of the ventilation pocket was not noticeably changed in the Polyox solutions from that in water.

The height of the spray was reduced by the polymer additive. This reduction increased as the polymer concentration increased. Concentrations of 100 wppm of Polyox caused a 10% decrease in the height of spray compared to water; and 200 wppm concentrations caused reduction of approximately 30% of the water value.

Thus, although greatly altering the appearance of the surface wake of cylinders, the Polyox solutions changed the spray height only a small amount, and the pocket depth very little, if at all. Further investigations into this problem are necessary to isolate those factors affecting the surface wake.

GRAPH 1

WATER

VENTILATION DEPTH OF CYLINDERS

20

18

16

14

12

h_{po}
(cm)

23

$F_h = 14$

$F_h = 1.8$

APPENDIX A

GRAPHS

x 1/4" DIA.

o 1/2" DIA.

□ 1" DIA.

△ 2" DIA.

7

6

5

$V^2 \left(\frac{cm}{sec} \right)^2 \times 10^{-4}$

3

2

1

0

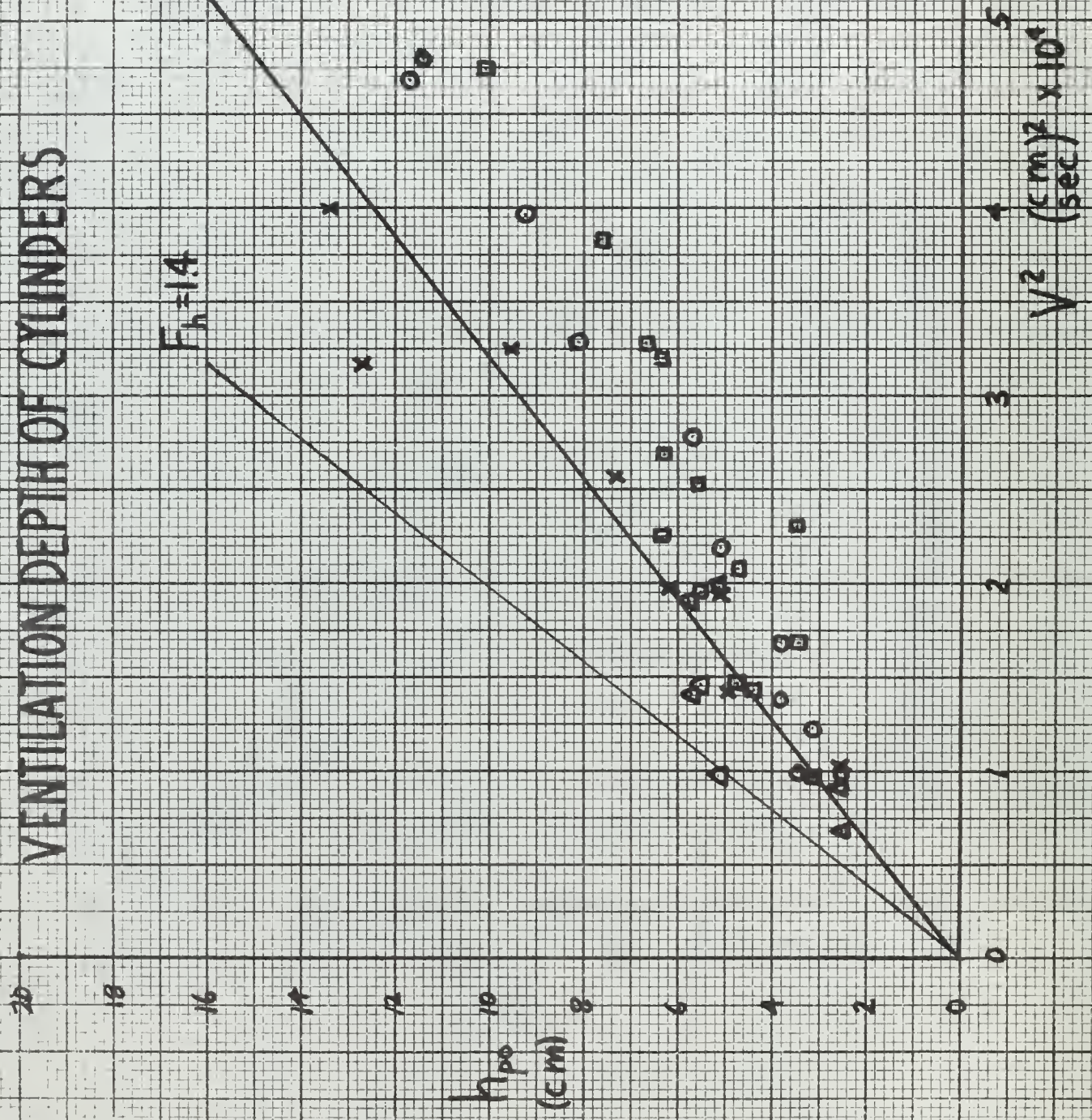
VENTILATION DEPTH OF CYLINDERS

GRAPH 2
POLYOX 100 WPPM

$F_h = 1.8$

$F_h = 1.4$

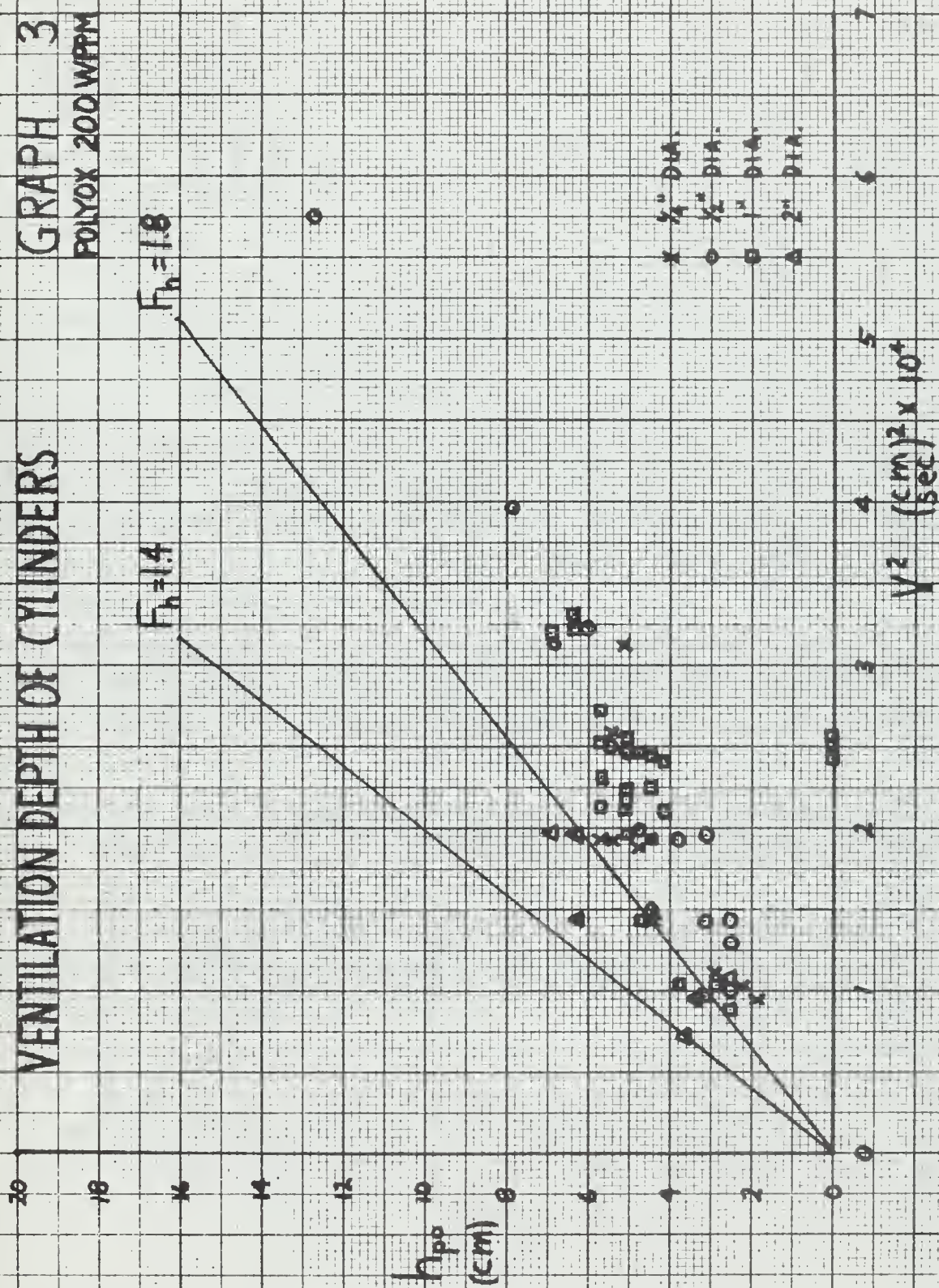
- X 1/4" DIA.
- 1/2" DIA.
- 1" DIA.
- △ 2" DIA.



VENTILATION DEPTH OF CYLINDERS

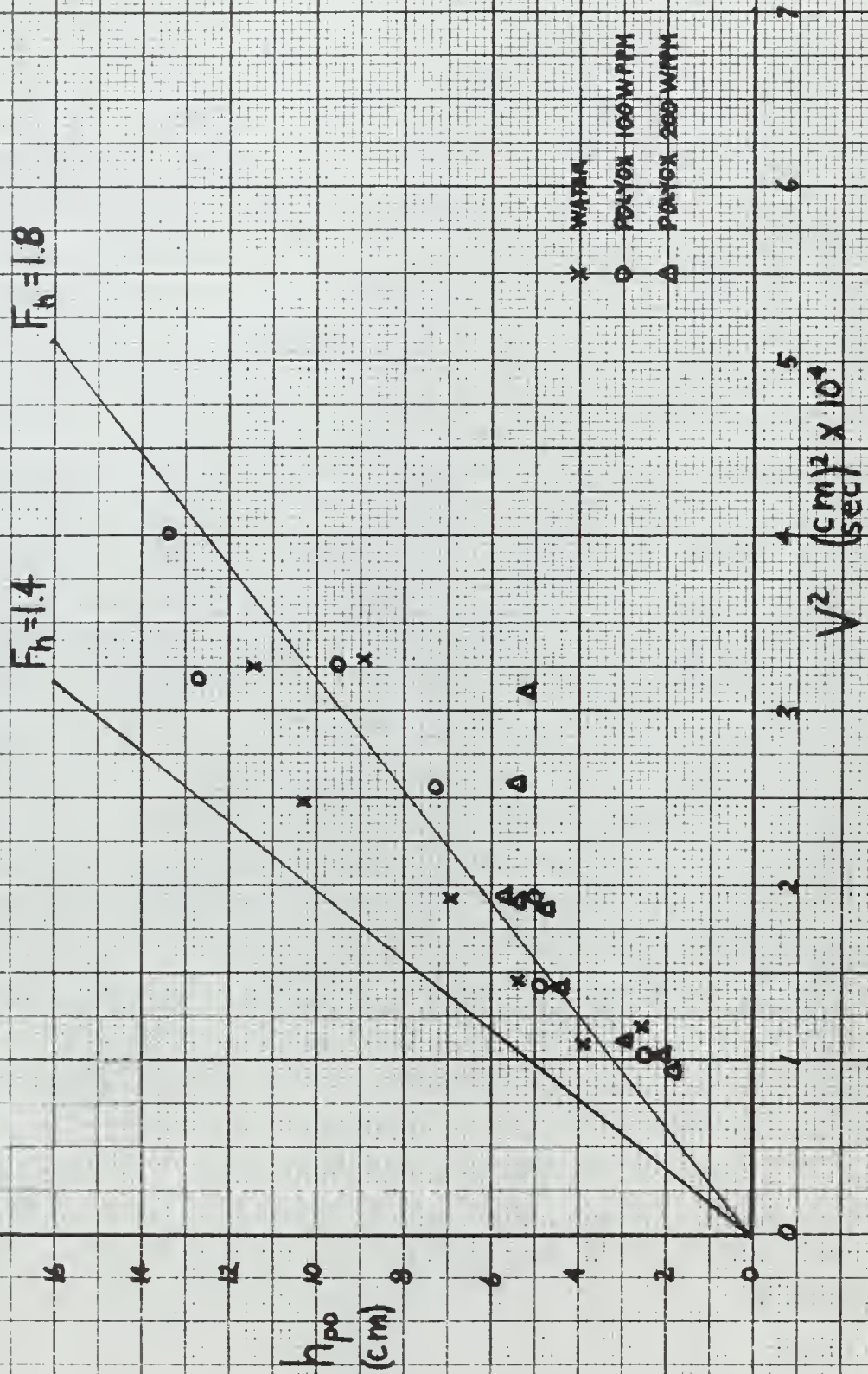
GRAPH 3

POLYOX 200 WPPM



VENTILATION DEPTH OF CYLINDERS

GRAPH 4
1/4" DIA.



VENTILATION DEPTH OF CYLINDERS

GRAPH 5
1/2" DIA.

$F_h = 14$ $F_h = 18$

h_{po}
(cm)

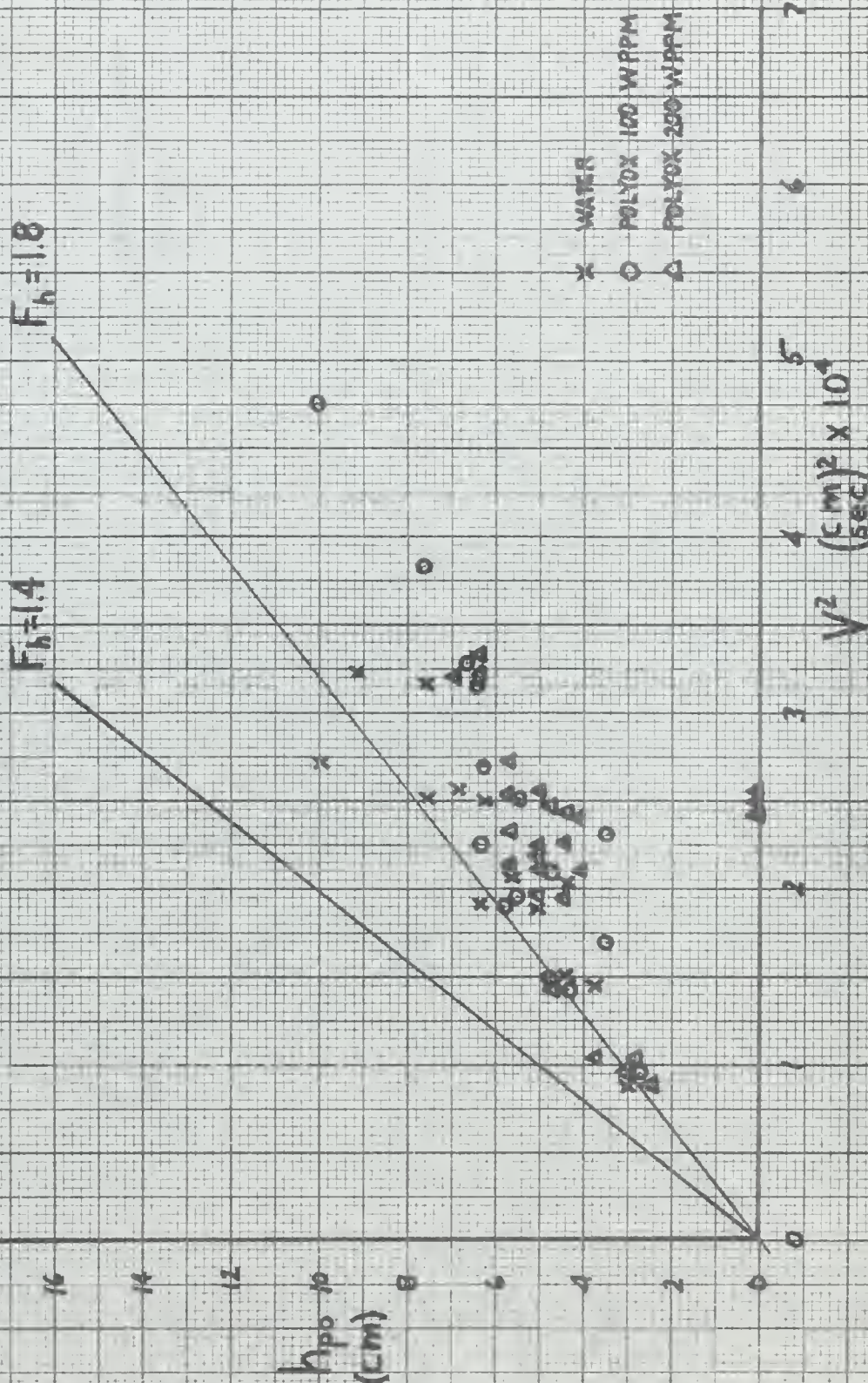
$V^2 \text{ (cm/sec)}^2 \times 10^4$

x WATER
o POLYOX 100 WPPM
Δ POLYOX 500 WPPM

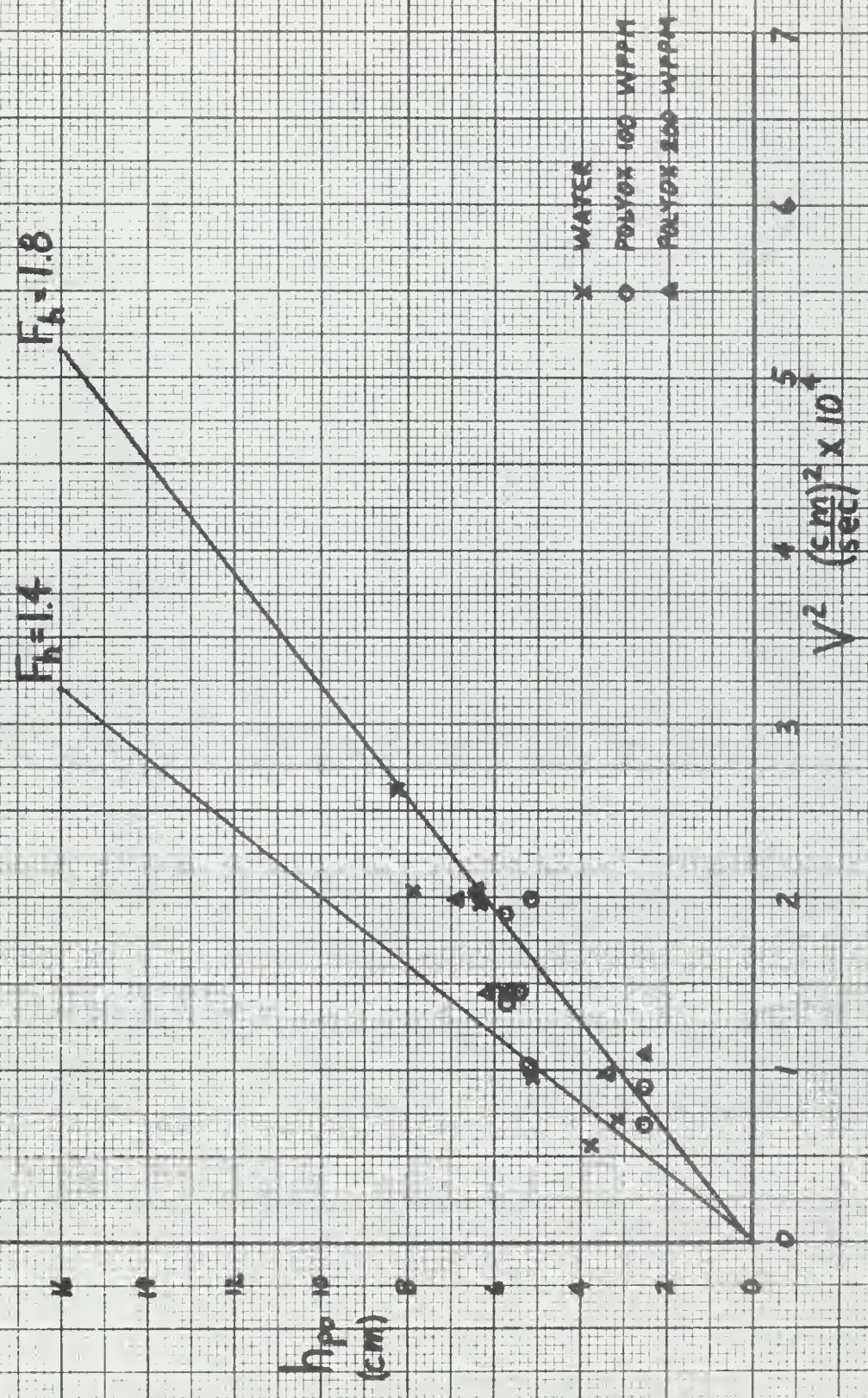
VENTILATION DEPTH OF CYLINDERS

GRAPH 6

1" DIA.



VENTILATION DEPTH OF CYLINDERS GRAPH 7 2" DIA.



SPRAY HEIGHT OF CYLINDERS

GRAPH 8

WATER

x 1/4" DIA.
o 1/2" DIA.
□ 1" DIA.
Δ 2" DIA.

HOERNER
x 1/4" DIA.
o 1/2" DIA.
□ 1" DIA.
Δ 2" DIA.

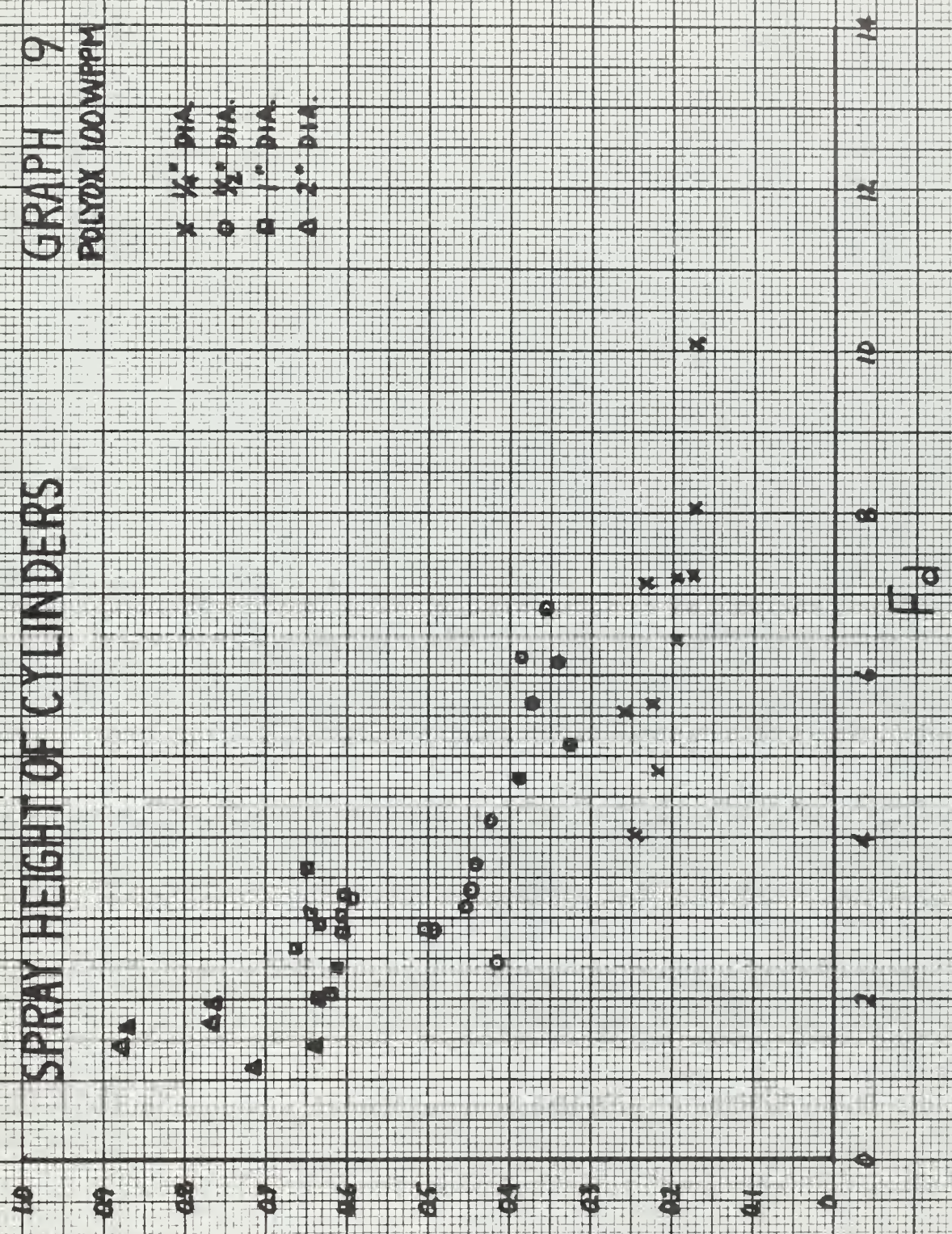
$$\frac{h_u}{V^2/2g}$$

F_d

GRAPH 9
POLYOX 100 WPPM

x 1/4" DIA.
o 1/2" DIA.
□ 1" DIA.
Δ 2" DIA.

SPRAY HEIGHT OF CYLINDERS

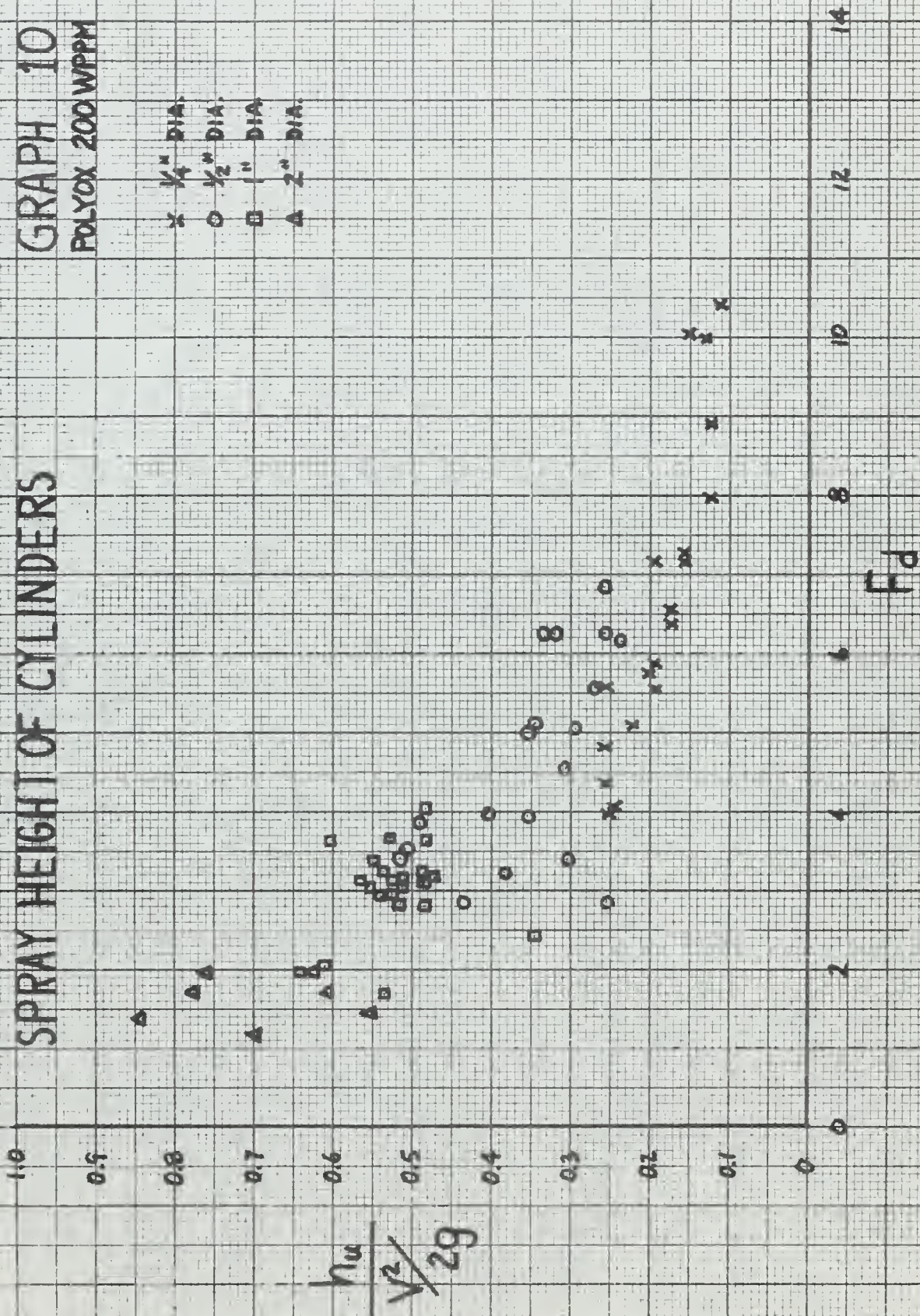


SPRAY HEIGHT OF CYLINDERS

GRAPH 10

POLYOX 200 WPPM

- x 1/4" DIA.
- o 1/2" DIA.
- 1" DIA.
- Δ 2" DIA.



SPRAY HEIGHT OF CYLINDERS

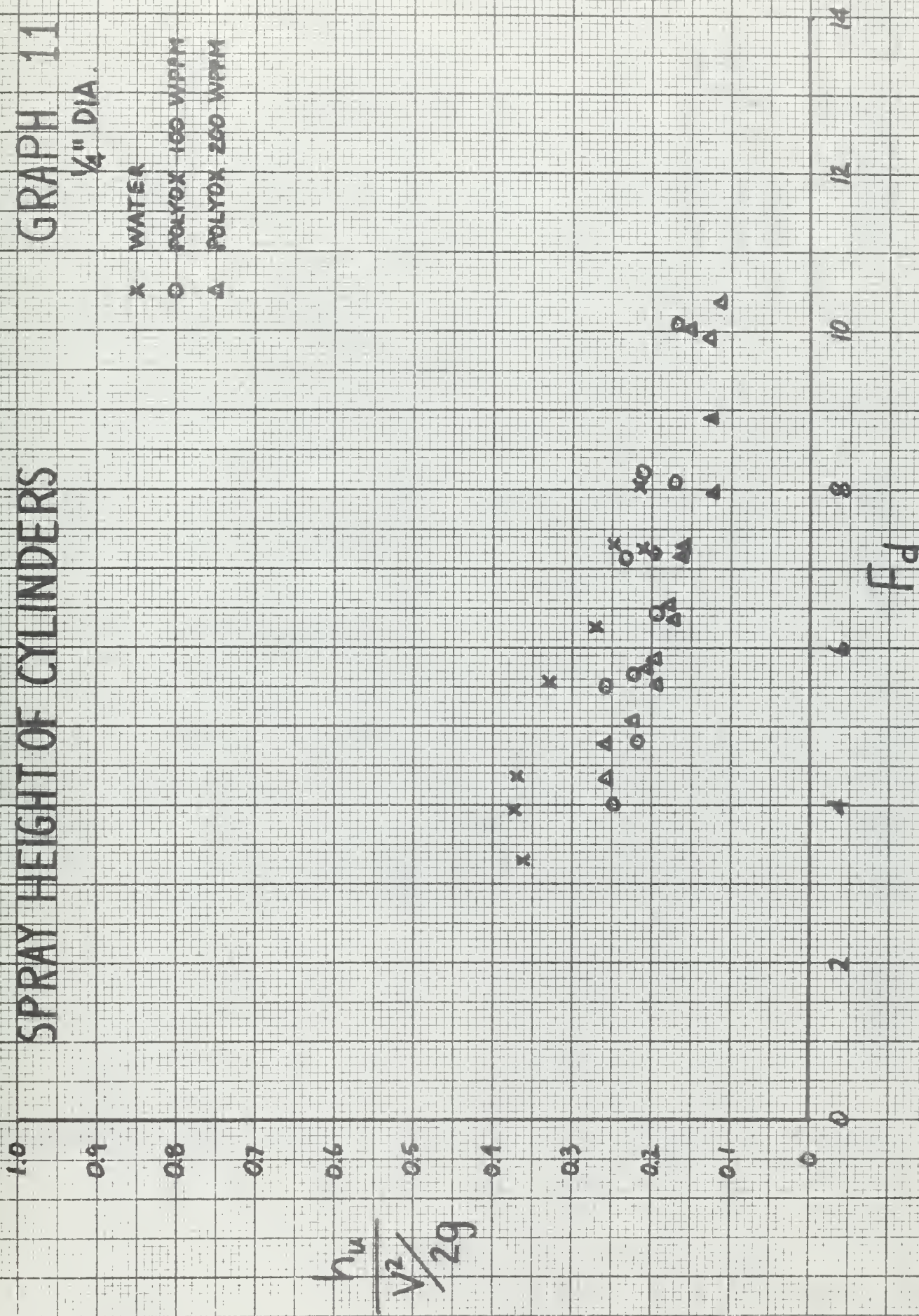
GRAPH 11

1/4" DIA.

x WATER

o POLYOX 100 WPPM

Δ POLYOX 200 WPPM



SPRAY HEIGHT OF CYLINDERS

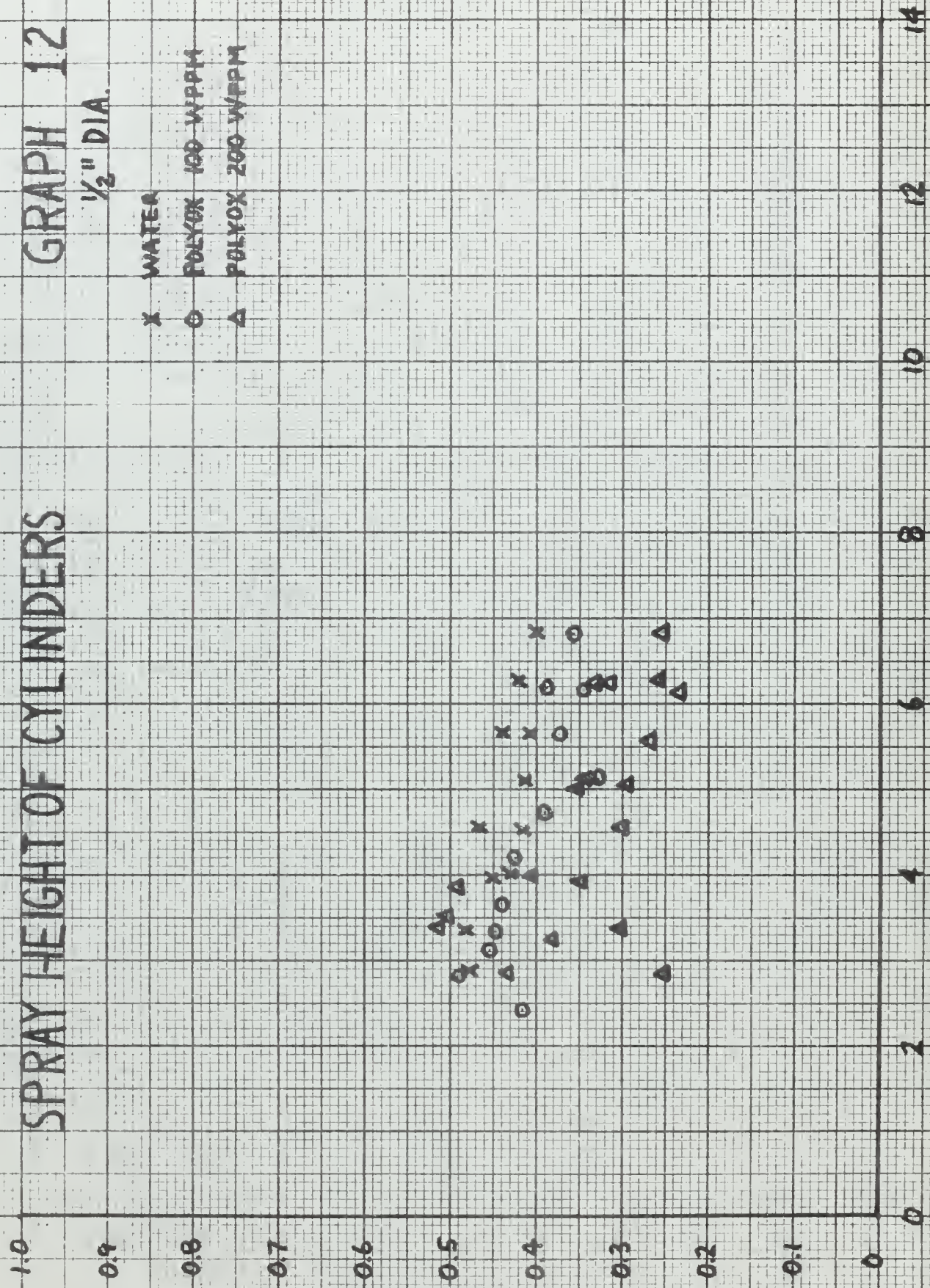
GRAPH 12

1/2" DIA.

- x WATER
- o POLYOX 100 WPPM
- Δ POLYOX 200 WPPM

$$\frac{h_u}{V^2/2g}$$

F_D

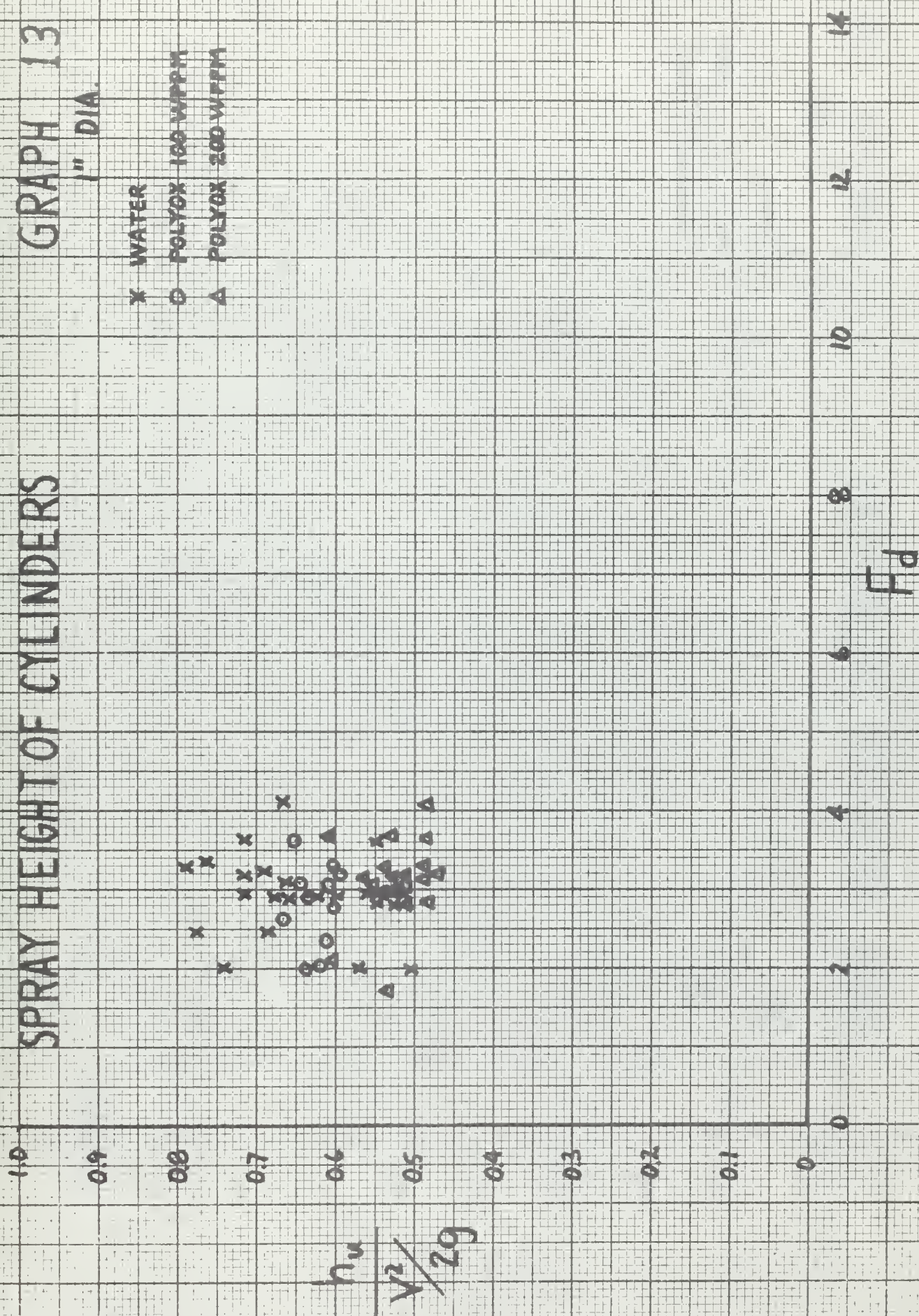


SPRAY HEIGHT OF CYLINDERS

GRAPH 13

1" DIA.

- x WATER
- o POLYOX 100 WPPM
- Δ POLYOX 200 WPPM

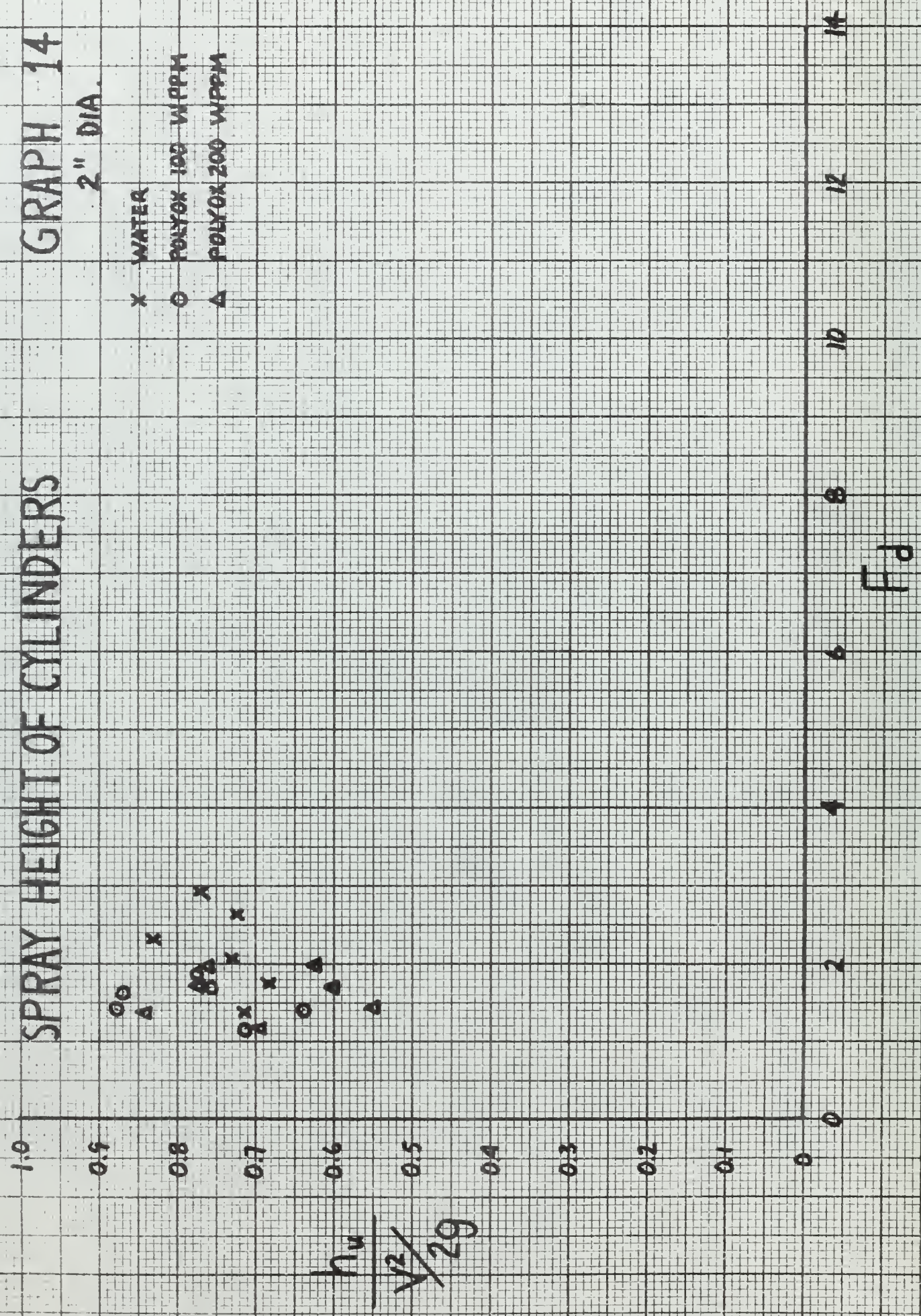


SPRAY HEIGHT OF CYLINDERS

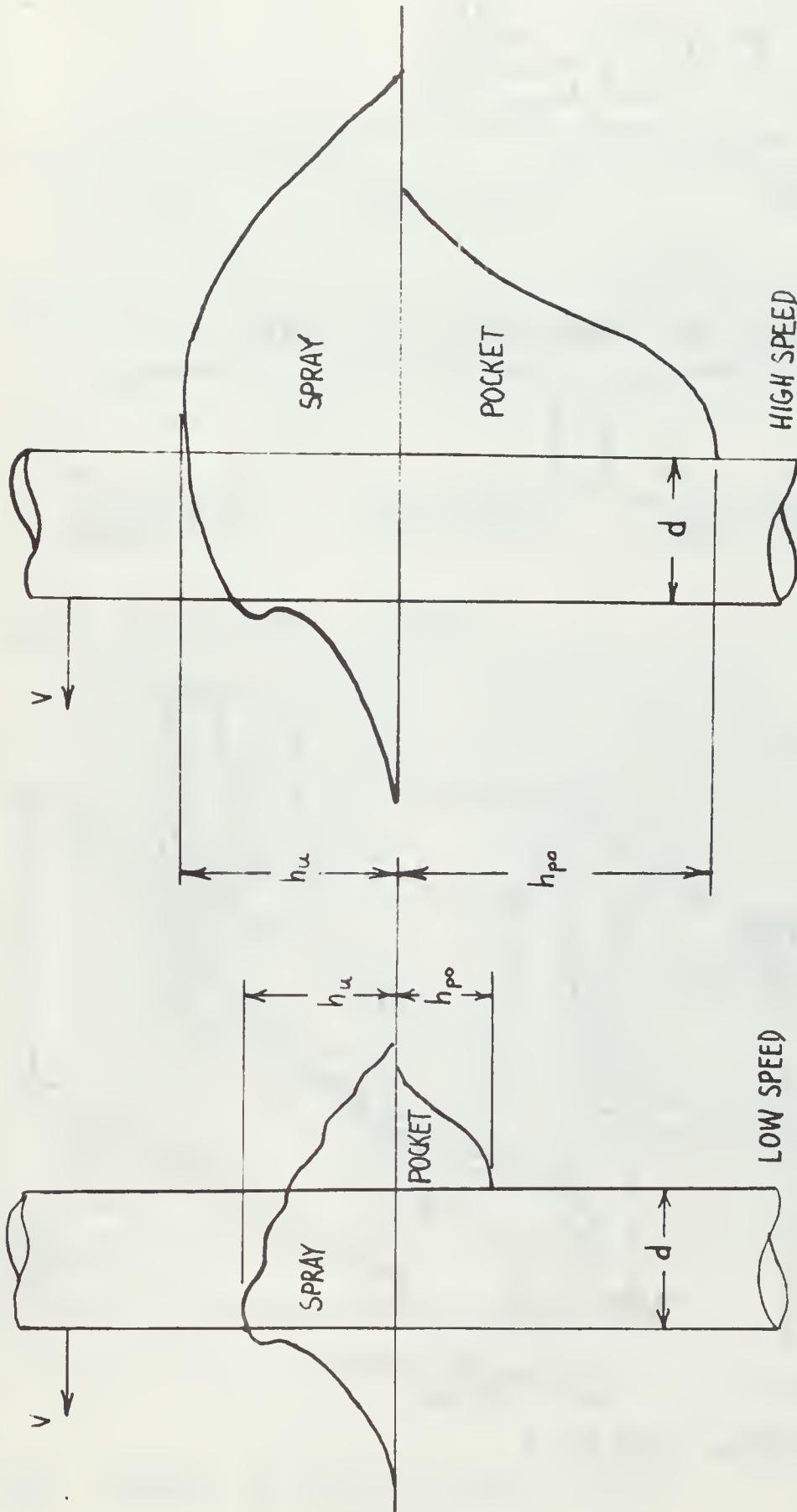
GRAPH 14

2" DIA.

- x WATER
- o POLYOK 100 WPPM
- Δ POLYOK 200 WPPM



FIGURES



$$F_h = \frac{V}{\sqrt{gh_{po}}} \quad F_d = \frac{V}{\sqrt{gd}}$$

FIG.1. WAKE PARAMETERS

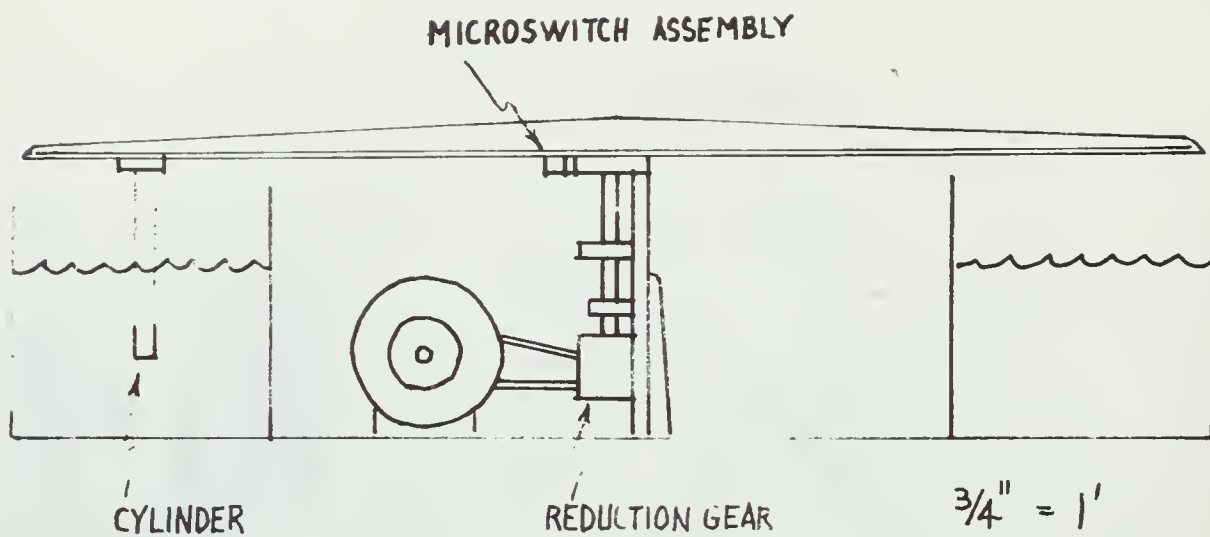


FIG.2 CROSS SECTIONAL VIEW OF TANK

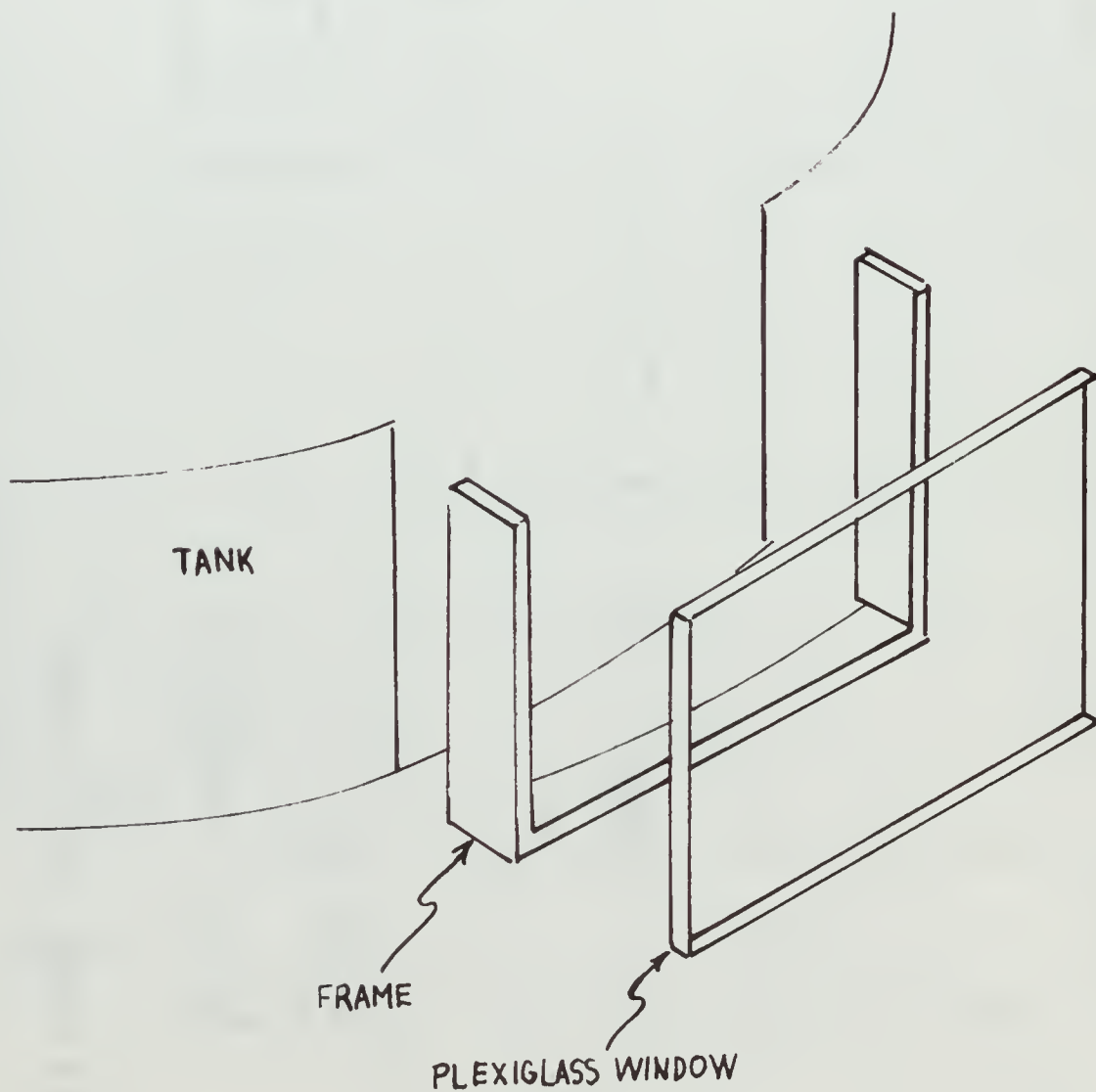


FIG.3 WINDOW ASSEMBLY

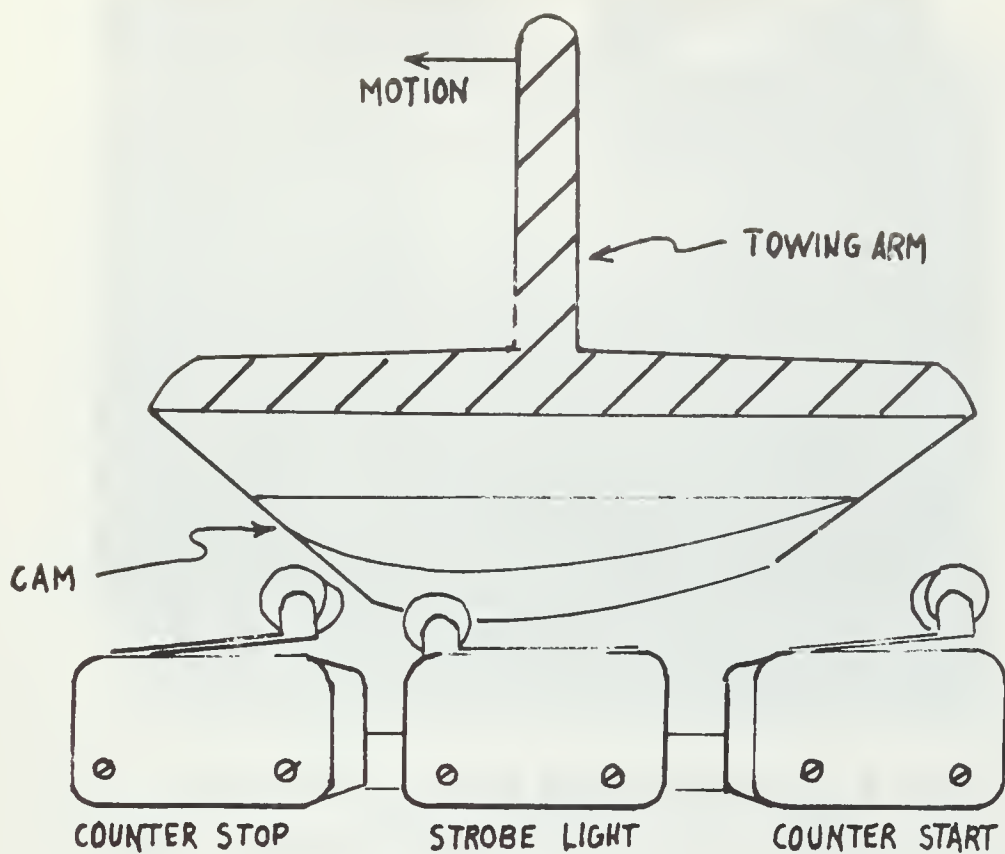


FIG.4. MICROSWITCH ASSEMBLY

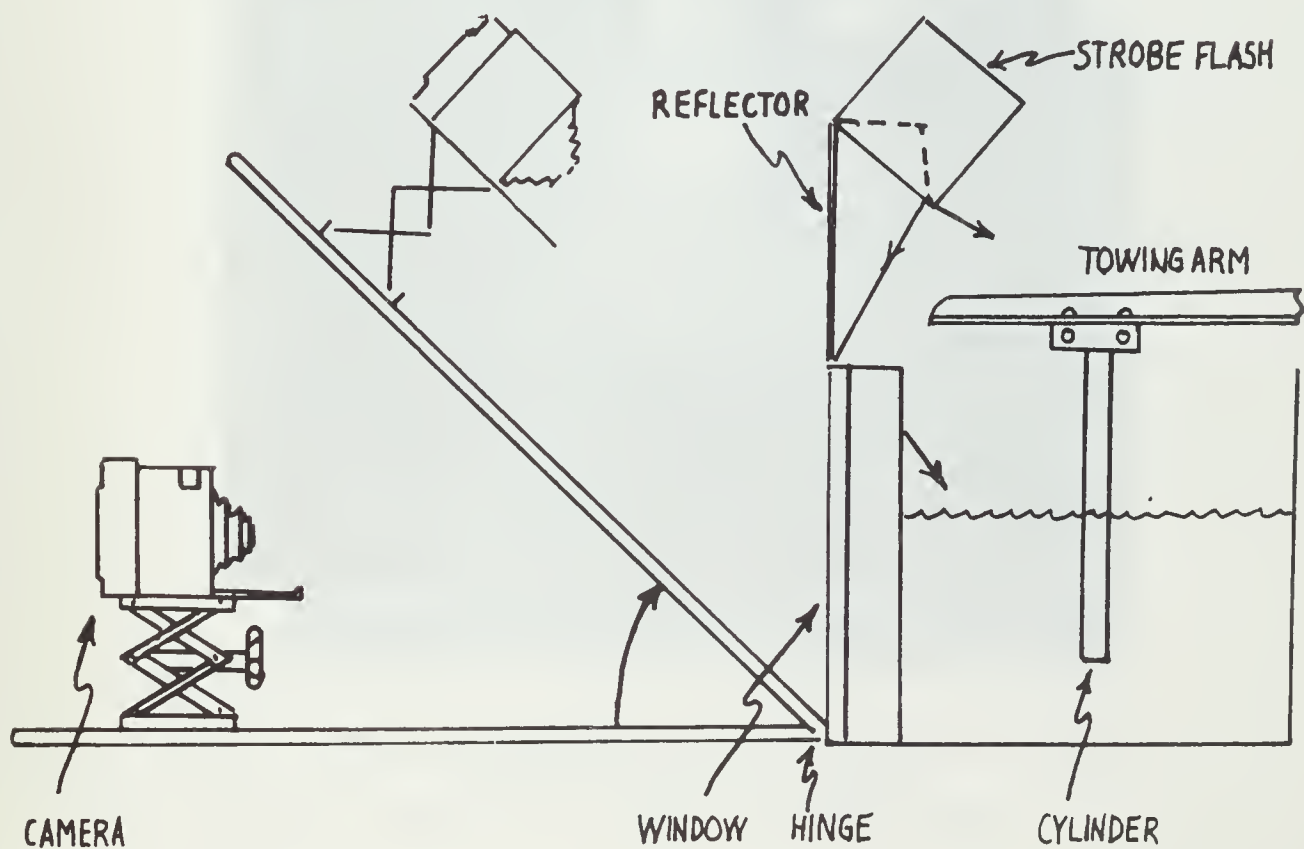


FIG.5 CAMERA AND STROBE FLASH MOUNTS

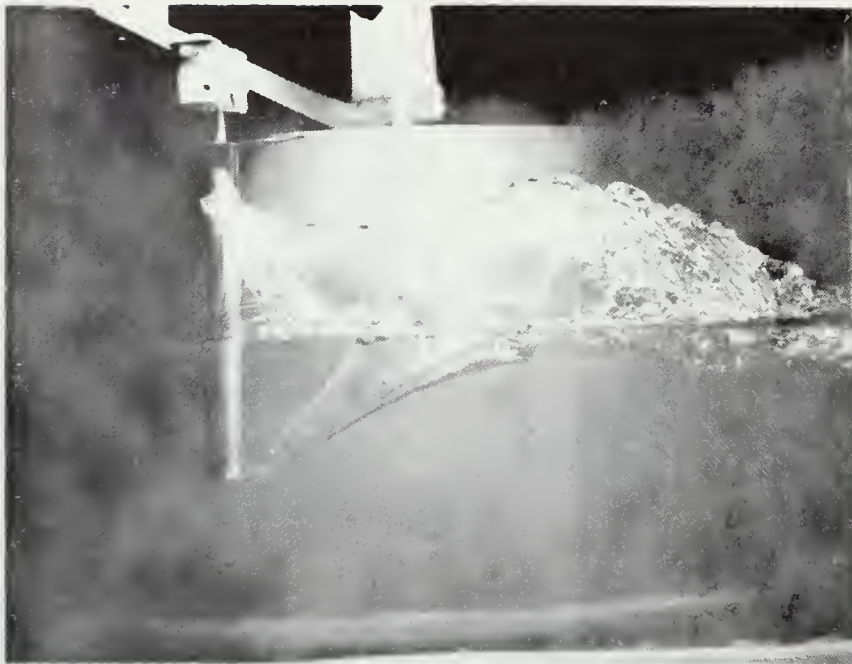


Fig. 6 Fully Developed Bottom Effect: Water,
 $d = 1$ in., $V = 183$ cm/sec.



Fig. 7 Beginning of Bottom Effect: Water,
 $d = 1$ in., $V = 150$ cm/sec.



Fig. 8 Water, $d = 2$ in., $V = 97.5$ cm/sec.



Fig. 9 Water, $d = 2$ in., $V = 142$ cm/sec.

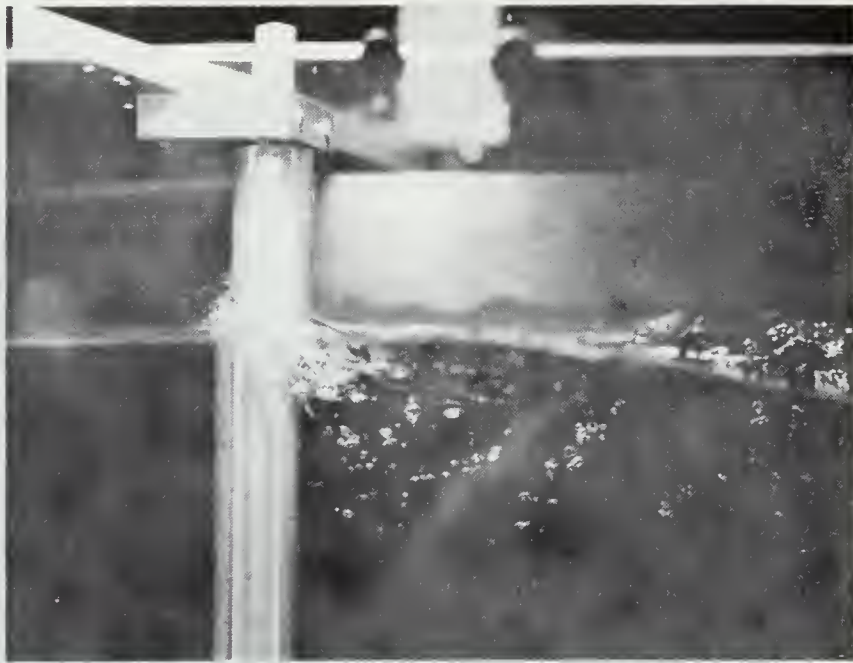


Fig. 10 Polyox 100 wppm, $d = 2$ in., $V = 99$ cm/sec.



Fig. 11 Poloyx 100 wppm, $d = 2$ in., $V = 139$ cm/sec.



Fig. 12 Polyox 200 wppm, $d = 2$ in., $V = 98$ cm/sec.

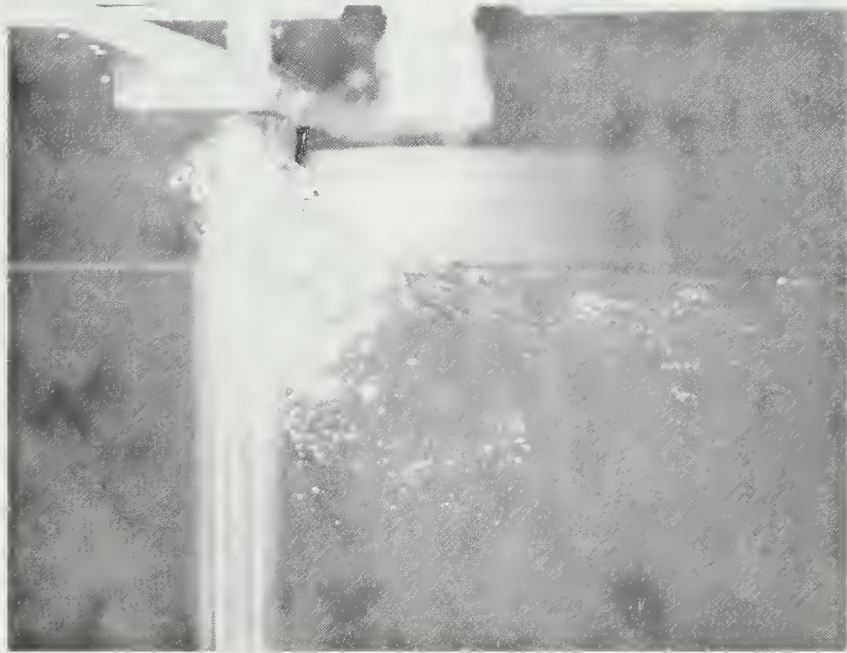


Fig. 13 Polyox 200 wppm, $d = 2$ in., $V = 140$ cm/sec.



Fig. 14 Water, $d = 1$ in., $V = 120$ cm/sec.

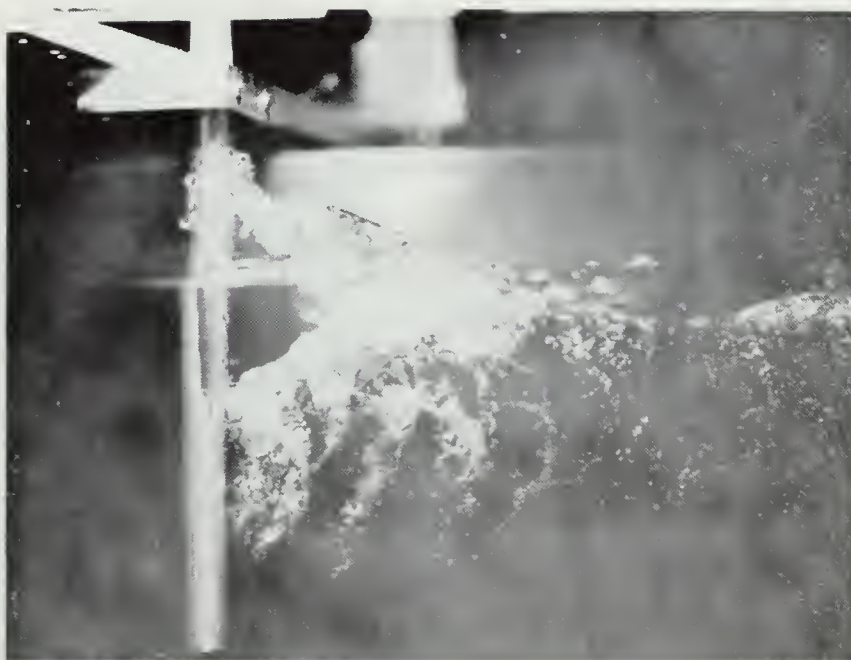


Fig. 15 Water, $d = 1$ in., $V = 159$ cm/sec.



Fig. 16 Polyox 100 wppm, $d = 1$ in., $V = 119$ cm/sec.

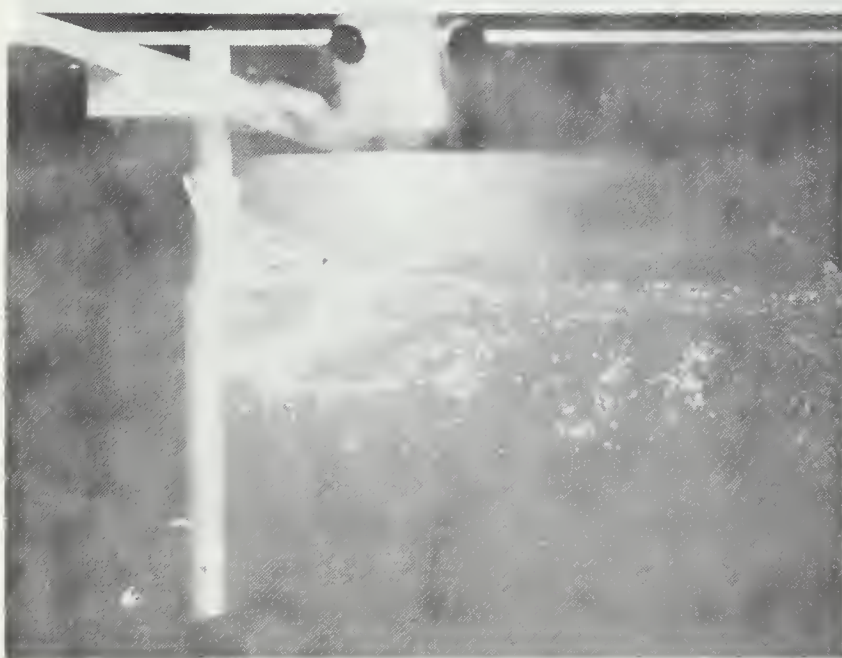


Fig. 17 Polyox 100 wppm, $d = 1$ in., $V = 159$ cm/sec.



Fig. 18 Polyox 200 wppm, $d = 1$ in., $V = 120$ cm/sec.

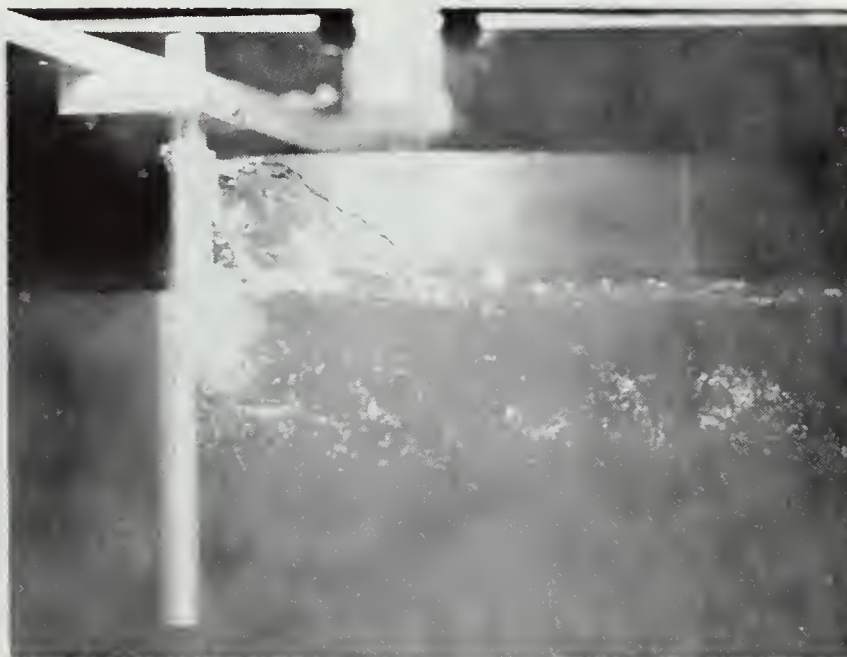


Fig. 19 Polyox 200 wppm, $d = 1$ in., $V = 200$ cm/sec.



Fig. 20 Absence of Ventilation Pocket
Polyox 200 wppm, $d = 1$ in., $V = 156$ cm/sec.

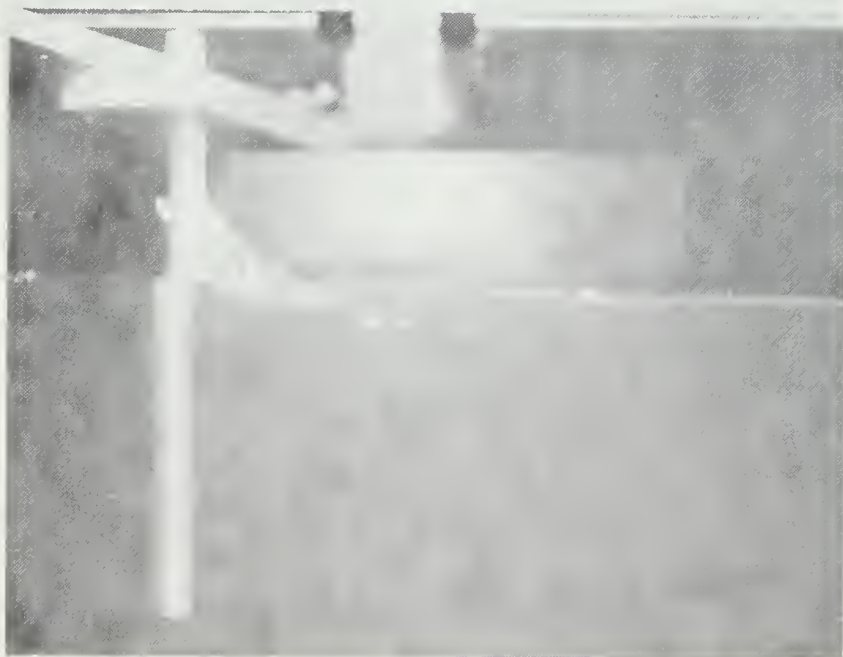


Fig. 21 Absence of Ventilation Pocket, Polyox
200 wppm, $d = 1$ in., $V = 160$ cm/sec.

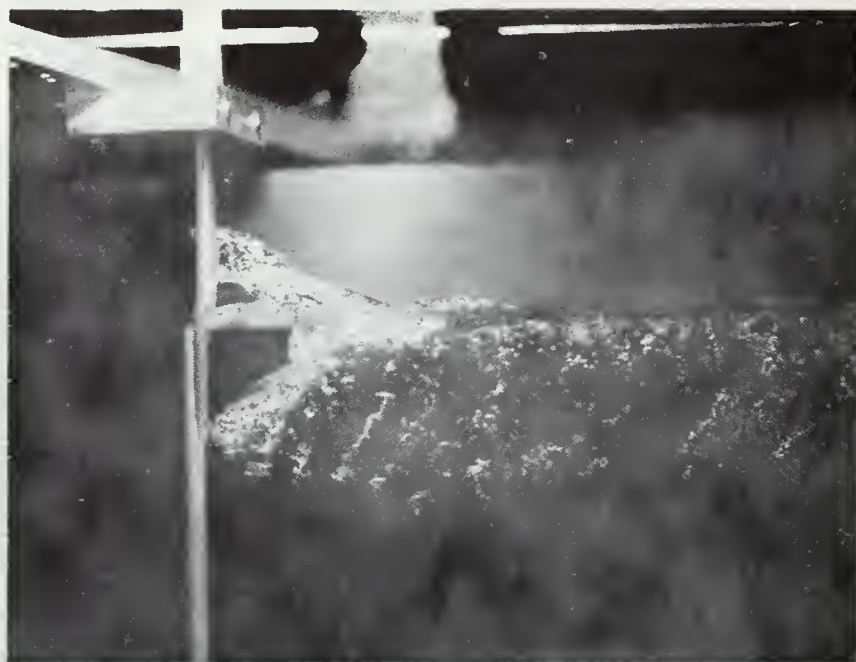


Fig. 22 Water, $d = 1/2$ in., $V = 159$ cm/sec.

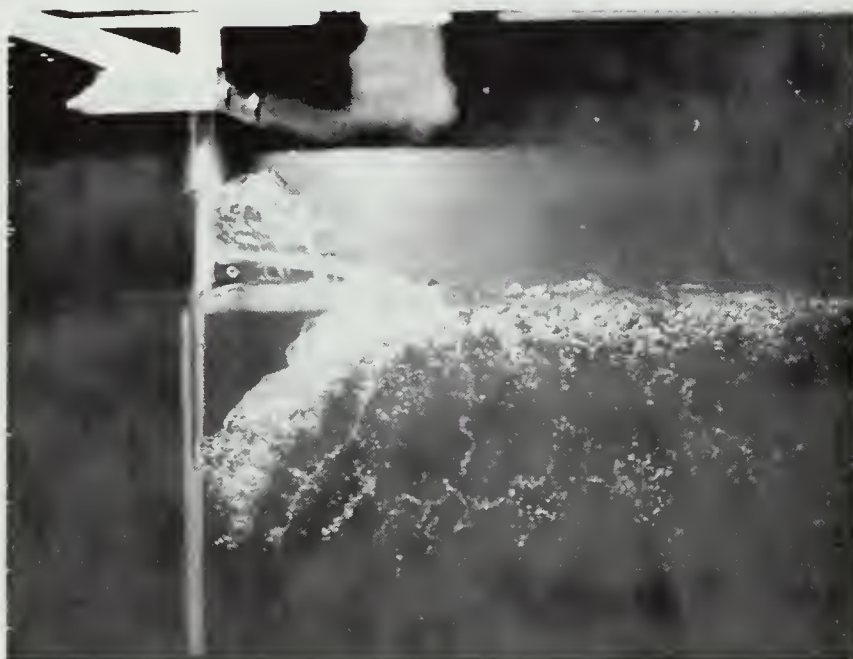


Fig. 23 Water, $d = 1/2$ in., $V = 202$ cm/sec.

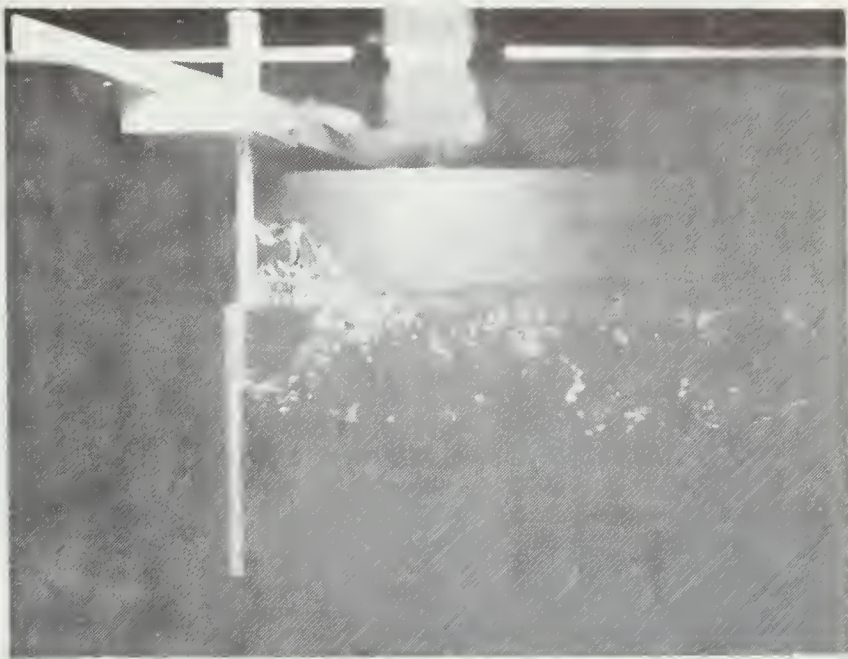


Fig. 24 Polyox 100 wppm, $d = 1/2$ in., $V = 166$ cm/sec.

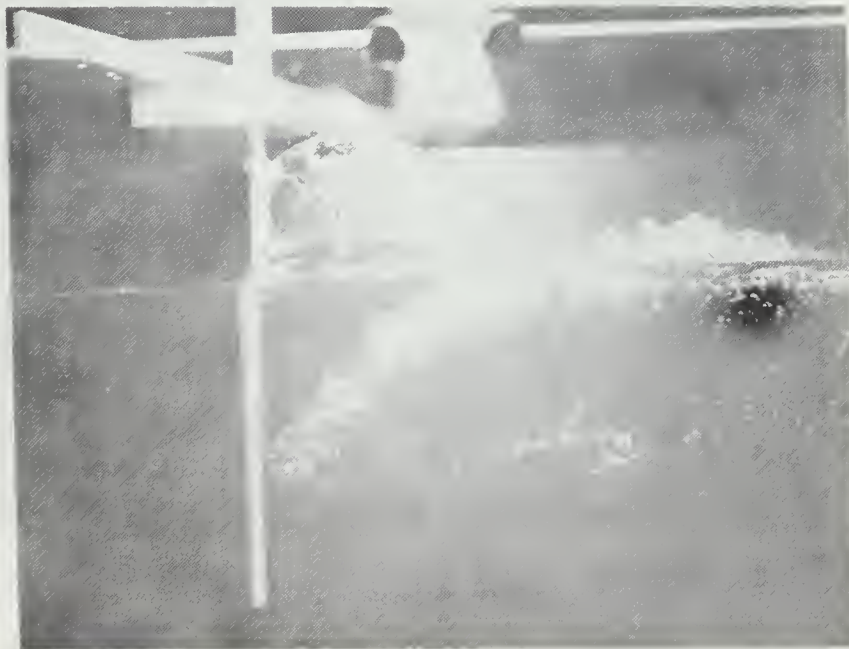


Fig. 25 Polyox 100 wppm, $d = 1/2$ in., $V = 219$ cm/sec.

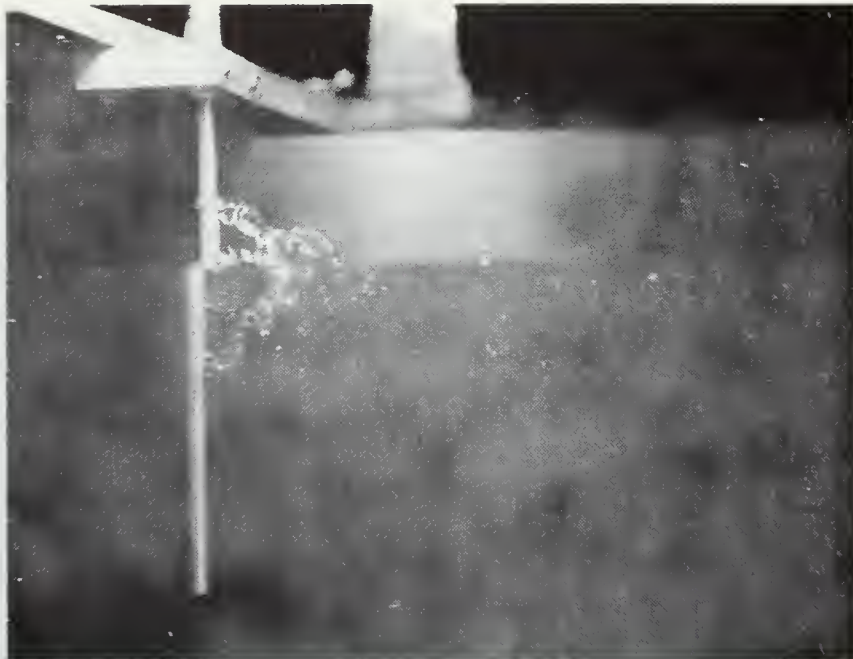


Fig. 26 Polyox 200 wppm, $d = 1/2$ in., $V = 178$ cm/sec.

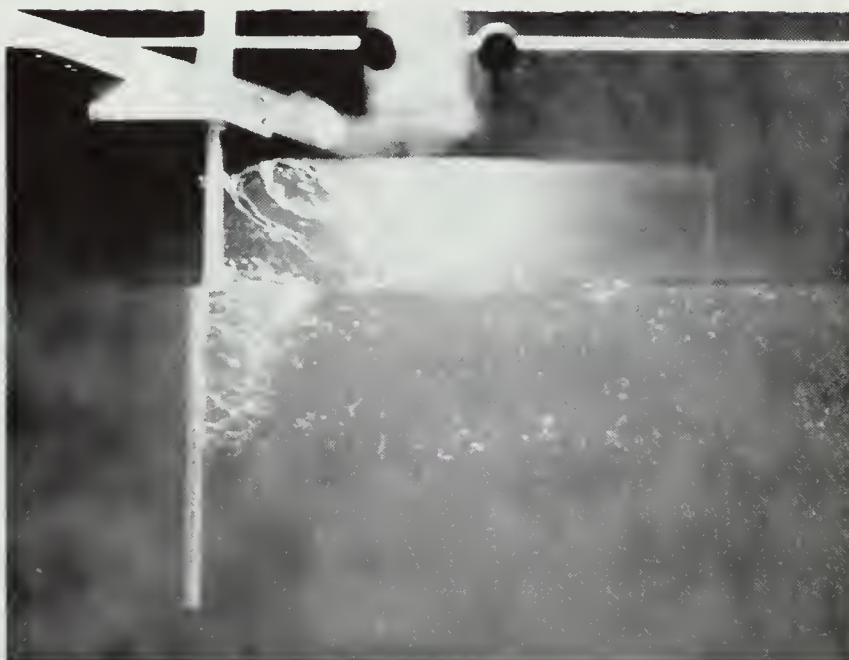


Fig. 27 Polyox 200 wppm, $d = 1/2$ in., $V = 221$ cm/sec.

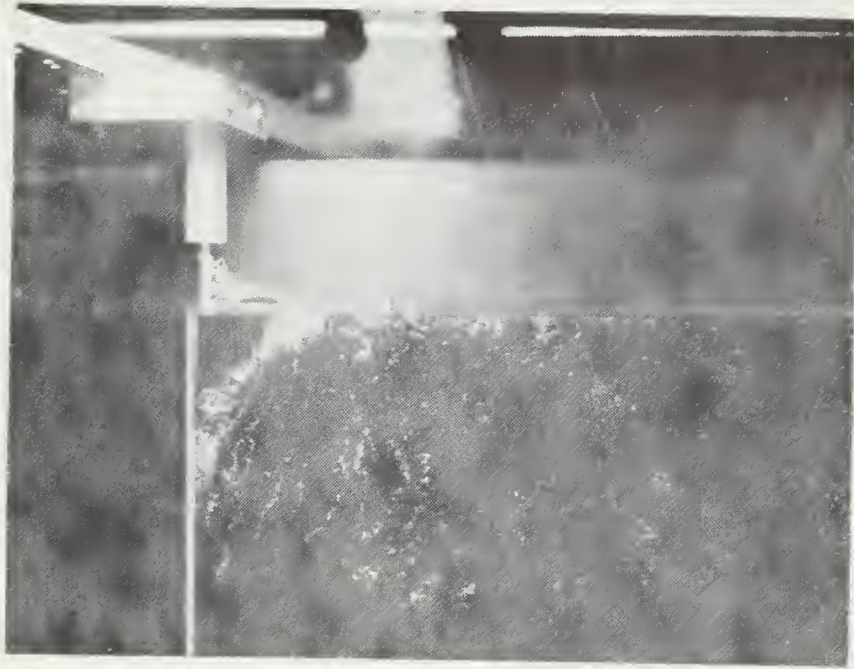


Fig. 28 Water, $d = 1/4$ in., $V = 157$ cm/sec.

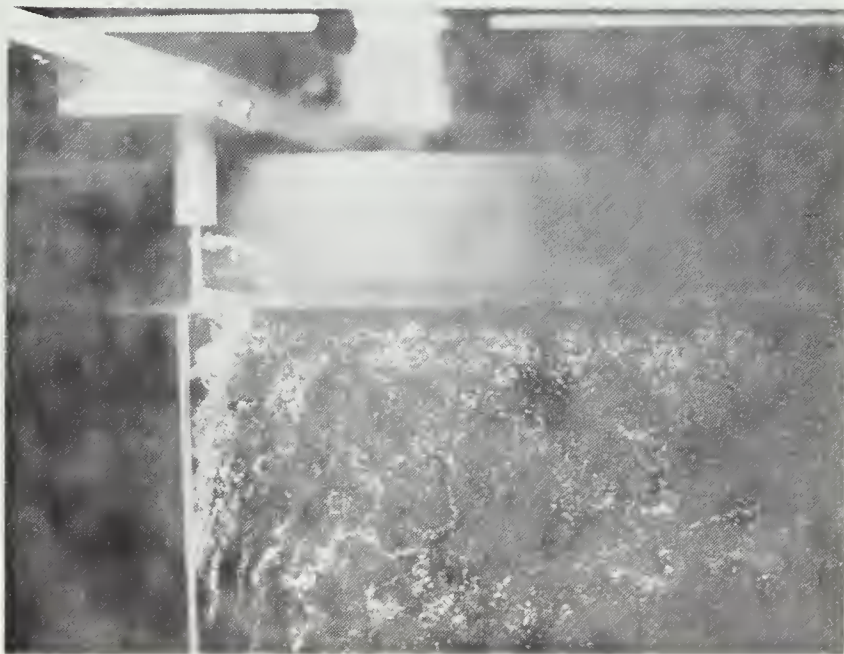


Fig. 29 Water, $d = 1/4$ in., $V = 200$ cm/sec.

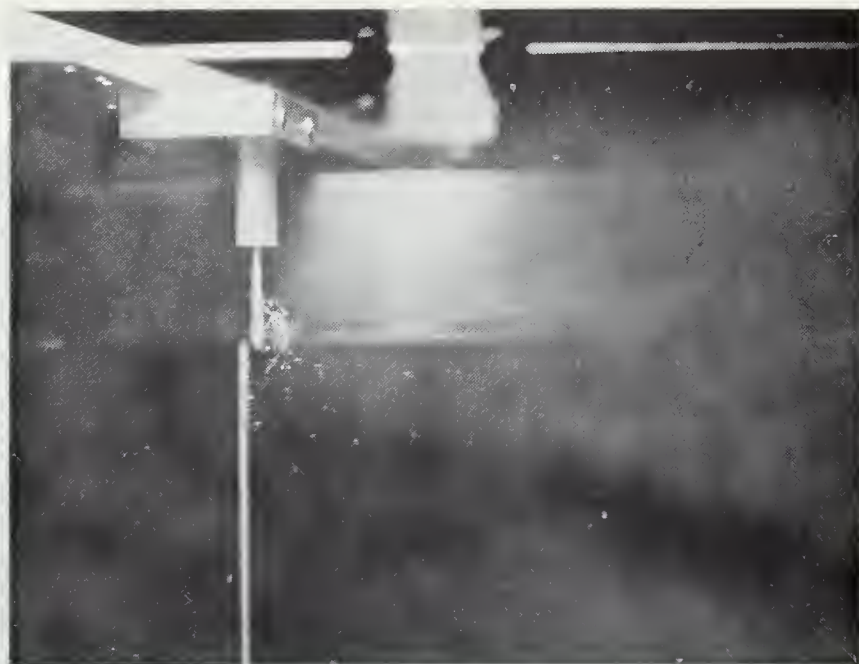


Fig. 30 Polyox 100 wppm, $d = 1/4$ in., $V = 141$ cm/sec.

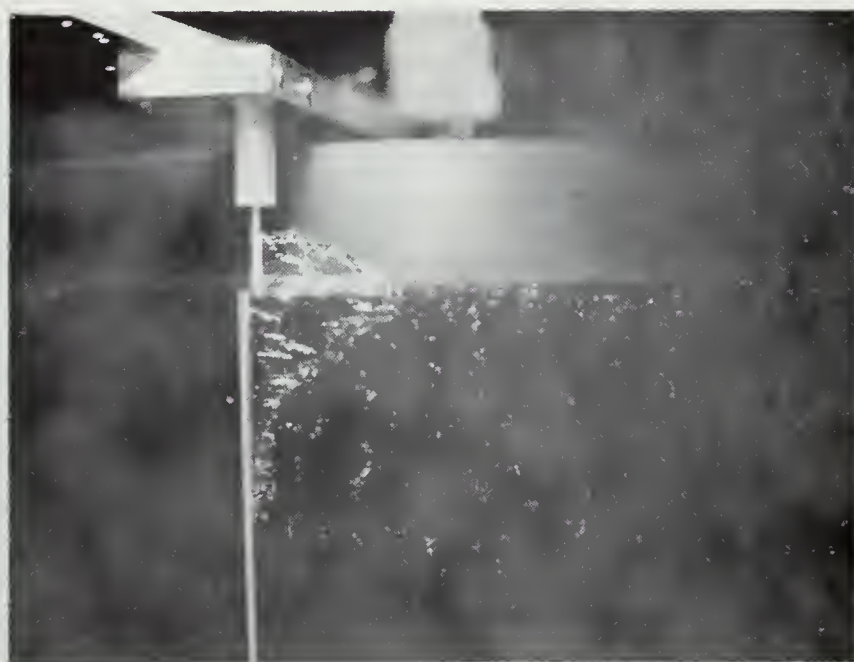


Fig. 31 Polyox 100 wppm, $d = 1/4$ in., $V = 200$ cm/sec.

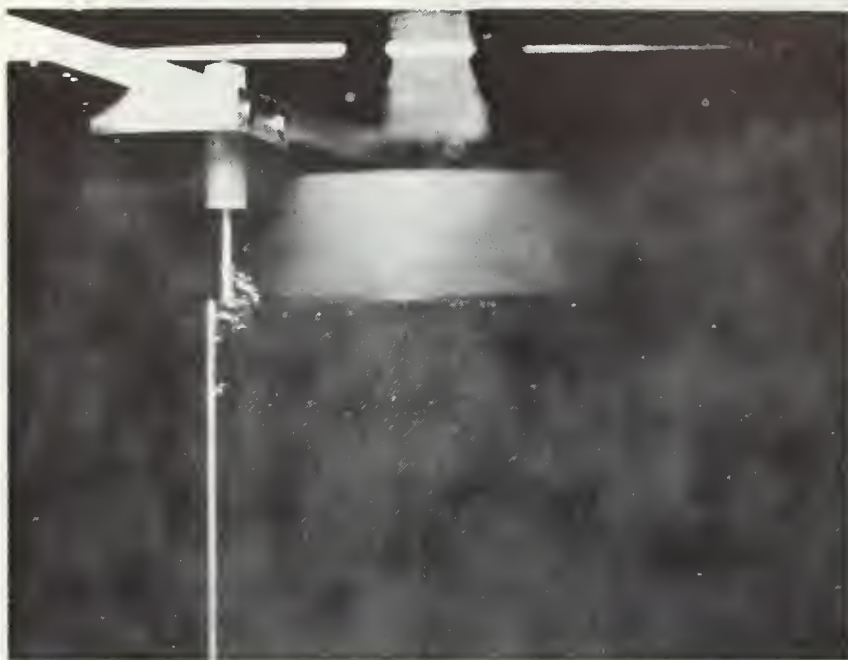


Fig. 32 Polyox 200 wppm, $d = 1/4$ in., $V = 140$ cm/sec.

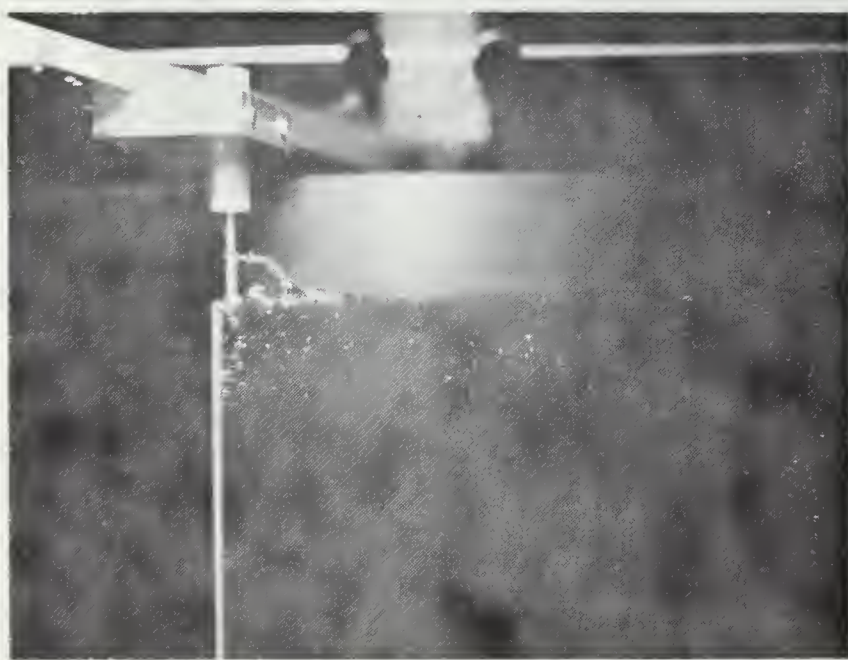


Fig. 33 Polyox 200 wppm, $d = 1/4$ in., $V = 198$ cm/sec.

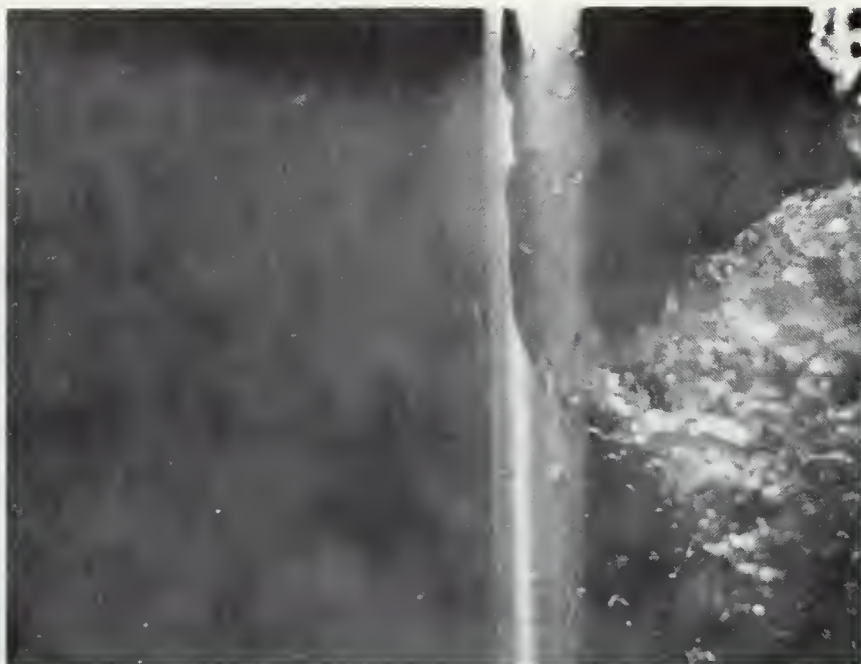


Fig. 34 Separation Line in Water, $d = 1$ in.,
 $V = 165$ cm/sec.

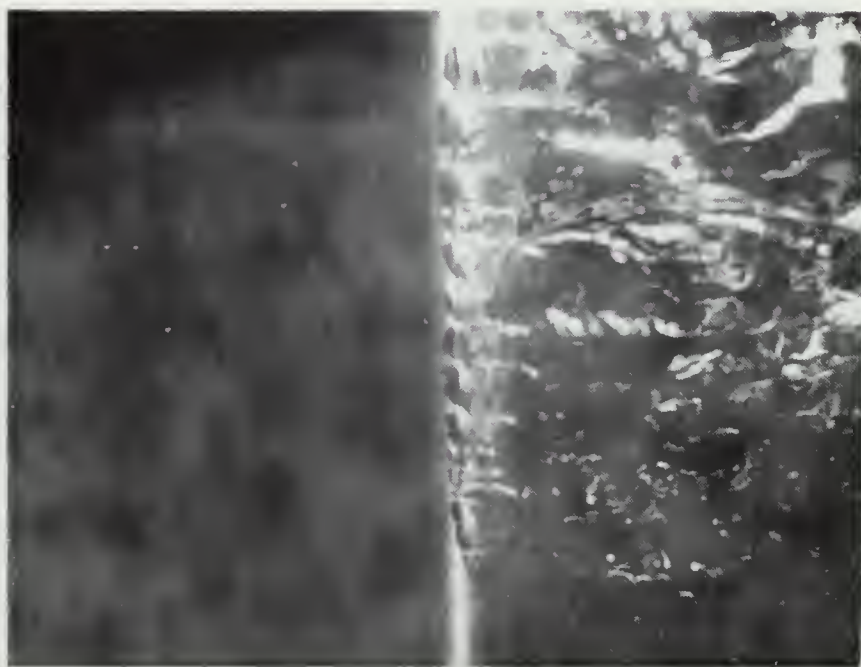


Fig. 35 Separation Line in 100 wppm Polyox,
 $d = 1$ in., $V = 179$ cm/sec.

BIBLIOGRAPHY

1. Toms, B. A., "Some Observations on the Flow of Linear Polymer Solutions Through Straight Tubes at Large Reynolds Numbers," Proceedings of the International Rheological Congress, Scheveningen, Holland, 1948.
2. Dodge, D. W. and Metzner, A. B., "Turbulent Flow of Non-Newtonian Systems," A.I.Ch.E.J. 5, 189 (1959).
3. Elata, C. and Tirosh, J., "Frictional Drag Reduction," Isreal Journal of Technology, 3, 1 (1965).
4. Elata, C., Lehrer, J. and Kahanovitz, A., "Turbulent Shear Flow of Polymer Solutions," Isreal Journal of Technology, 4, 87 (1966).
5. Fabula, A. G., "The Toms Phenomenon in the Turbulent Flow of Very Dilute Polymer Solutions," Fourth International Congress on Rheology (John Wiley and Sons, Inc., New York, 1965).
6. Hershey, H. C., "Drag Reduction in Newtonian Polymer Solutions," Ph. D. Thesis, University of Missouri, Rolla, 1965.
7. Hershey, H. C. and Zakin, J. L., "A Study of Turbulent Drag Reduction of Solutions of High Polymers in Organic Solvents," Symposium on Mechanics of Viscoelastic Fluids, A.I.Ch.E., Philadelphia, Pa.
8. Patterson, G. K., "Turbulence Measurements in Polymer Solutions Using Hot Film Anemometry," Ph. D. Thesis, University of Missouri, Rolla, 1966.
9. Patterson, G. K. and Zakin, J. L., "Hot Film Anemometry Measurements of Turbulence in Pipe Flow: Organic Solvents," A.I.Ch.E.J. 13, 513 (1967).
10. Pruitt, G. T. and Crawford, H. R., "Effect of Molecular Weight and Segmental Constitution on the Drag Reduction of Water Soluble Polymers," Rept. DTMB-1, The Western Co., 1965.
11. Ripkin, J. F. and Pilch, M., "Non-Newtonian Pipe Friction Studies with Various Dilute Polymer Water Solutions," Project Report 71, St. Anthony Falls Hydraulic Laboratory, University of Minnesota, 1964.
12. Savins, J. G., "Drag Reduction Characteristics of Macromolecules in Turbulent Pipe Flow," Symposium on Non-Newtonian Fluid Mechanics, 56th Annual A.I.Ch.E. Meeting, Houston, Texas, 1963.

13. Shaver, R. G. and Merrill, E. W., Turbulent Flow of Pseudo-plastic Polymer Solutions in Straight Cylindrical Tubes," A.I.Ch.E.J. 2, 181 (1959).
14. Virk, P. S., "The Toms Phenomenon-Turbulent Pipe Flow of Dilute Polymer Solutions," Ph. D. Thesis, Massachusetts Institute of Technology, 1966.
15. Wells, C. S. and Spangler, J. G., "Effects of Local Injection of a Drag Reducing Fluid into Turbulent Pipe Flow of a Newtonian Fluid," Fourth Winter Meeting of the Society of Rheology, 1967.
16. Merrill, E. W., "Turbulent Flow of Polymer Solutions," Progress Report, Dept. of Chemical Engineering, Massachusetts Institute of Technology, April, 1965.
17. Hoyt, J. W. and Fabula, A. G., "The Effect of Additives on Fluid Friction," NOTS TP 3670, Naval Ordnance Test Station, China Lake, California, December, 1964.
18. Vogel, W. M. and Patterson, A. M., "An Experimental Investigation of the Effect of Additives Injected into the Boundary Layer of an Underwater Body," Fifth Symposium on Naval Hydrodynamics, Bergen, Norway, 1965.
19. Baronet, C. N. and Hoppmann, W. H., "Drag Reduction Causes by Polymer Solutions Injected into the Water Flowing Around Cylindrical Bodies," Technical Report, Dept. of Mech. Eng., Rensselaer Poly. Institute, 1966.
20. Thurston, S. and Jones, R. D., "Experimental Model Studies of Non-Newtonian Soluble Coatings for Drag Reduction," J. Aircraft 2, 122 (1965).
21. Merrill, E. W., Smith, K. A., and Chung, Y. C., "Drag Augmentation by Polymer Addition," A.I.Ch.E. 12, 809 (1966).
22. Pruitt, G. T. and Crawford, H. R., "Paper Presented at the Symposium on Non-Newtonian Fluid Mechanics," Houston, Texas, 1963.
23. Ruszczky, M. A., "Sphere Drop Tests in High Polymer Solutions," Nature 206, 614 (1965).
24. Lang, T. G. and Patrick, H. V. L., "Drag of Blunt Bodies in Polymer Solutions," NOTS TP 4379, Naval Ordnance Test Station, China Lake, California, July, 1967.
25. Sanders, J. V., "Drag Coefficients of Spheres in Poly(ethylene oxide) Solutions," Int. Shipbuilding Progress 14, 153 (1967).
26. Hayes, M. F., "Drag Coefficients of Spheres Falling in Dilute Aqueous Solutions of Long-Chain Macromolecules," Thesis, Naval Postgraduate School, Monterey, Calif., 1966.

27. Chenard, J. H., "Drag of Spheres in Dilute Aqueous Solutions of Poly(ethylene oxide) Within the Region of the Critical Reynolds Number," Thesis, Naval Postgraduate School, Monterey, Calif., 1967.
28. James, D. G., "Laminar Flow of Dilute Polymer Solutions Around Circular Cylinders," Thesis, Calif. Inst. of Technology, Pasadena, Calif., 1967.
29. McClanahan, T. and Ridgely, P. J., "Drag of Circular Cylinders in Dilute Aqueous Solutions of Poly(ethylene oxide) for Flows Characterized by Laminar Boundary Layer Separation," Thesis, Naval Postgraduate School, Monterey, Calif., 1968.
30. Shin, H., "Reduction of Drag in Turbulence by Dilute Polymer Solutions," SC. D. Thesis, Massachusetts Inst. of Technology, 1965.
31. Gadd, G. E., "Turbulence Damping and Drag Reduction Produced by Certain Additives in Water," Nature, 206, 463 (1965).
32. Ellis, A. T., "Some Effects of Macromolecules on Cavitation Inception and Noise," Division of Eng. and App. Science, Calif. Inst. of Technology, Pasadena, Calif., 1967.
33. Hoerner, S. F., "Some Characteristics of Spray and Ventilation," ONR Tech. Report 15, (1953).
34. Brennan, C., "Some Cavitation Experiments with Dilute Polymer Solutions," von Kármán Laboratory, Calif. Inst. of Technology, Pasadena, Calif., 1968.
35. Brennan, C., Conversation with the author. Naval Postgraduate School, Monterey, California, 1969.

INITIAL DISTRIBUTION LIST

	No. Copies
1. Defense Documentation Center Cameron Station Alexandria, Virginia 22314	20
2. Library, Code 0212 Naval Postgraduate School Monterey, California 93940	2
3. Chief of Naval Research Office of Naval Research Washington, D. C. 20360	1
4. Professor James V. Sanders, Code 61 Sd Department of Physics Naval Postgraduate School Monterey, California 93940	5
5. LT(jg) Michael H. Fletcher U. S. Naval Nuclear Power School Mare Island Naval Shipyard Vallejo, California 94592	3
6. Mr. Bill Smith Department of Physics Naval Postgraduate School Monterey, California 93940	1
7. Dr. J. W. Hoyt Head of Propulsion Division Naval Undersea Warfare Center 3202 E. Foothill Blvd. Pasadena, California 91107	1
8. Dr. A. G. Fabula Naval Undersea Warfare Center 3202 E. Foothill Blvd. Pasadena, California 91107	1
9. Professor G. W. Rodeback, Code 61 Rk Department of Physics Naval Postgraduate School Monterey, California 93940	1
10. Dr. C. Brennan von Karman Laboratory California Inst. of Technology Pasadena, California	1

DOCUMENT CONTROL DATA - R & D

(Security classification of title, body of abstract and indexing annotation must be entered when the overall report is classified)

ORIGINATING ACTIVITY (Corporate author) Naval Postgraduate School Monterey, California 93940	2a. REPORT SECURITY CLASSIFICATION Unclassified 2b. GROUP
--	---

REPORT TITLE
Surface Wake of a Circular Cylinder in Dilute Aqueous Solutions of Poly(ethylene oxide)

DESCRIPTIVE NOTES (Type of report and inclusive dates)
Master's Thesis, June 1969

AUTHOR(S) (First name, middle initial, last name)
Michael H. Fletcher

REPORT DATE June 1969	7a. TOTAL NO. OF PAGES 59	7b. NO. OF REFS 35
--------------------------	------------------------------	-----------------------

9a. CONTRACT OR GRANT NO. b. PROJECT NO. c. d.	9a. ORIGINATOR'S REPORT NUMBER(S) 9b. OTHER REPORT NO(S) (Any other numbers that may be assigned this report)
---	--

10. DISTRIBUTION STATEMENT
Distribution of this document is unlimited.

11. SUPPLEMENTARY NOTES	12. SPONSORING MILITARY ACTIVITY Naval Postgraduate School Monterey, California 93940
-------------------------	---

13. ABSTRACT

The wake formed by surface-piercing circular cylinders towed through 0, 100, and 200 parts per million (by weight) aqueous solutions of Poly(ethylene oxide), Polyox WSR-301, was examined photographically. Cylinder diameters ranged from 1/4 in. to 2 in.; Froude numbers from 0.6 to 10. Measurements of spray height and ventilation pocket depth were made. No significant alteration of pocket depth with polymer concentration was observed; however, the spray height was reduced by increasing the Polyox concentration. Qualitative differences between the wakes of cylinders in Polyox solutions and those in water were (1) a serrated separation line characterized the ventilation pocket of the polymer solutions as opposed to the straight separation line of water, (2) the striated appearance of the pocket walls in Polyox instead of the clear, smooth walls in water, (3) the coherence displayed by the spray in Polyox instead of the random character of the spray in water, and (4) the larger and more irregularly shaped bubbles in Polyox as opposed to those in water.

KEY WORDS

LINK A

LINK B

LINK C

ROLE

WT

ROLE

WT

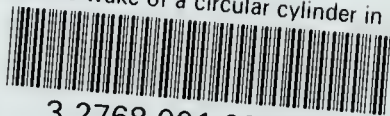
ROLE

W 7

Spray height and ventilation pocket depth

thesF5216

Surface wake of a circular cylinder in d



3 2768 001 99255 5

DUDLEY KNOX LIBRARY